

**CHONG ZHI KAI**

**B. ENG (HONS) CHEMICAL ENGINEERING**

**SEPTEMBER 2015**

**EFFECT OF MODEL-PLANT MISMATCH ON MODEL  
PREDICTIVE CONTROL AND MISMATCH THRESHOLD  
DETERMINATION**

**CHONG ZHI KAI**

**CHEMICAL ENGINEERING  
UNIVERSITI TEKNOLOGI PETRONAS  
SEPTEMBER 2015**

**Effect of Model-Plant Mismatch on Model Predictive Control  
and Mismatch Threshold Determination**

by

Chong Zhi Kai

15379

Dissertation submitted in partial fulfillment of  
the requirements for  
Bachelor of Engineering (Hons)  
(Chemical Engineering)

SEPTEMBER 2015

Universiti Teknologi PETRONAS,  
32610, Bandar Seri Iskandar,  
Perak.

CERTIFICATION OF APPROVAL

**Effect of Model-Plant Mismatch on Model Predictive Control and Mismatch  
Threshold Determination**

by

Chong Zhi Kai  
15397

A project dissertation submitted to the  
Chemical Engineering Programme  
Universiti Teknologi PETRONAS  
in partial fulfillment of the requirement for the  
BACHELOR OF ENGINEERING (Hons)  
(CHEMICAL ENGINEERING)

Approved by,

---

(Dr Lemma Dendena Tufa)

UNIVERSITI TEKNOLOGI PETRONAS  
BANDAR SERI ISKANDAR, PERAK

September 2015

## CERTIFICATION OF ORIGINALITY

This is to certify that I am responsible for the work submitted in this project, that the original work is my own except as specified in the references and acknowledgements, and that the original work contained herein have not been undertaken or done by unspecified sources or persons.

---

(Chong Zhi Kai)

## ABSTRACT

The performance of model predictive control is highly affected by model-plant mismatch. Existing model-plant mismatch detection, isolation and estimation techniques do not take into account the threshold of significant mismatch, preventing clear analysis of the implications of mismatch. This study investigates the relationship between model-plant mismatch and plant performance in a multiple input multiple output system and determines the thresholds of mismatch. The approach uses a closed loop system with the Wood and Berry distillation model controlled by MPC simulated with varying degrees of parametric mismatch. The threshold values above which the MPC performance is unacceptable are determined from the Integral Error- MPM graph by specifying the base Integral Error. The values for positive mismatches are 27%, 19% 40% and 31% for the four gains, 27%, 40% 40% and 32% for the time constants and 21%, 9%, 6% and 14% for the time delays respectively. The values for negative mismatches are 22%, 22% 38% and 16% for the four gains, 20%, 20% 31% and 20% for the time constants and 40%, 10%, 6% and 11% for the time delays respectively. Time delay mismatch yields the most significant effect on the MPC performance. Gain mismatch causes significant impact on the MPC performance when the mismatch increases the condition number otherwise its impact is lower than the effect of time delay mismatch. The effect of mismatch in time constant becomes significant when the plant time constant increases, otherwise, it is minimal. Simultaneous mismatches in two transfer functions are pronounced when the mismatches affect the same output.

## **ACKNOWLEDGEMENTS**

I would like to thank Dr Lemma Dendena Tufa for his guidance and care as my supervisor in my final year project, without which I would certainly not have achieved as much.

# TABLE OF CONTENTS

<b>CERTIFICATION OF APPROVAL</b> .....	ii
<b>CERTIFICATION OF ORIGINALITY</b> .....	iii
<b>ABSTRACT</b> .....	iv
<b>ACKNOWLEDGEMENTS</b> .....	v
<b>TABLE OF CONTENTS</b> .....	vi
<b>LIST OF FIGURES</b> .....	viii
<b>LIST OF TABLES</b> .....	ix
<b>CHAPTER 1: INTRODUCTION</b> .....	1
1.1 Background .....	1
1.2 Problem Statement .....	4
1.3 Objectives .....	4
1.4 Scope of Study .....	5
<b>CHAPTER 2: LITERATURE REVIEW</b> .....	6
2.1 Model Predictive Control (MPC) .....	6
2.2 Model Predictive Control Performance .....	8
2.3 Model-Plant Mismatch (MPM) .....	9
2.4 Detection and Isolation of Model-Plant Mismatch .....	10
2.5 Quantifying the Impact of MPC on MPM Performance .....	15
2.6 Process Re-identification .....	15
<b>CHAPTER 3: METHODOLOGY</b> .....	17
3.1 Tools and Software .....	17
3.2 Description of Methodology .....	18
3.2.1 Single Parameter mismatch .....	18
3.2.2 Double parameter mismatch .....	22
3.3 Key Milestones .....	23
3.4 Gantt Chart .....	24
<b>CHAPTER 4: RESULTS AND DISCUSSION</b> .....	26
4.1 Single Parameter Mismatch .....	26
4.1.1 Single gain mismatch .....	29
4.1.2 Single time constant mismatch .....	33

4.1.3	Single time delay mismatch .....	36
4.1.4	Single parameter mismatch threshold .....	39
4.2	Double Parameter Mismatch.....	42
4.2.1	Double gain mismatch.....	43
4.2.2	Double time constant mismatch .....	45
4.2.3	Double time delay mismatch.....	46
4.2.4	Gain and time constant mismatch interaction ...	48
4.2.5	Gain and time delay mismatch interaction .....	49
4.2.6	Time constant and time delay mismatch interaction .....	50
4.2.7	Double parameter mismatch threshold considerations .....	52
4.3	Results Summary.....	53
4.3.1	Single parameter mismatch .....	53
4.3.2	Double parameter mismatch.....	53
<b>CHAPTER 5:</b>	<b>CONCLUSION AND RECOMMENDATIONS .....</b>	<b>54</b>
5.1	Conclusion.....	54
5.2	Recommendations .....	55
<b>REFERENCES</b>	.....	<b>56</b>
<b>APPENDICES</b>	.....	<b>58</b>

## LIST OF FIGURES

Figure 1:	MPC response .....	2
Figure 2:	New MPM detection and isolation algorithm.....	3
Figure 3:	MPC Control Flow .....	7
Figure 4:	Process Flow .....	18
Figure 5:	Simulink model block flow diagram .....	19
Figure 6:	Threshold determination example .....	22
Figure 7:	Key Milestones for May 2015 Semester .....	23
Figure 8:	Key Milestones for September 2015 Semester.....	23
Figure 9:	Gantt chart (FYP I) .....	24
Figure 10:	Gantt chart (FYP II).....	25
Figure 11:	Gain11 mismatch IAE, ITAE and ISE .....	27
Figure 12:	Gain22 mismatch IAE, ITAE and ISE. ....	28
Figure 13:	Plant response for 0% mismatch.....	29
Figure 14:	Condition numbers for gain mismatch .....	31
Figure 15:	Plant response for +40% Gain11 mismatch.....	32
Figure 16:	Plant response for -40% Gain11 mismatch .....	32
Figure 17:	Tau11 mismatch IAE .....	33
Figure 18:	Plant response for -40% Tau11 mismatch.....	35
Figure 19:	Plant response for +40% Tau11 mismatch .....	35
Figure 20:	Delay11 mismatch IAE.....	36
Figure 21:	Output response for -35% Delay22 mismatch.....	38
Figure 22:	Output response for -40% Delay22 mismatch.....	38
Figure 23:	Mismatch thresholds .....	39
Figure 24:	Gain11 and Gain12 mismatch IAE.....	43
Figure 25:	Gain11 and Gain21 mismatch IAE.....	44
Figure 26:	Tau11 and Tau12 mismatch IAE.....	45
Figure 27:	Delay11 and Delay12 mismatch IAE .....	46
Figure 28:	Gain11 and Tau11 mismatch IAE .....	48
Figure 29:	Gain11 and Tau12 mismatch IAE .....	49
Figure 30:	Gain21 and Delay22 mismatch IAE .....	50
Figure 31:	Tau21 and Delay22 mismatch IAE.....	51

## LIST OF TABLES

Table 1:	Summary of literature for controller performance measurement ....	9
Table 2:	Transfer function based techniques .....	14
Table 3:	Variable based and model based validation techniques .....	14
Table 4:	Tools and software.....	17
Table 5:	Simulation settings.....	20
Table 6:	Sample of mismatch matrix .....	20
Table 7:	Gain mismatch threshold .....	40
Table 8:	Time constant mismatch threshold .....	40
Table 9:	Time delay mismatch threshold.....	41

# CHAPTER 1

## INTRODUCTION

### 1.1 Background

Controllers are essential in most industries because of their critical role in controlling real processes that are dynamic in nature. This dynamics stems from naturally unstable inputs that deviate from the ideal steady state condition, the presence of disturbances and changing environmental conditions. In the presence of dynamics, controllers control the manipulated variables in order to ensure that the critical outputs of the process (product composition, product quality etc.) do not stray too far from the specifications.

Model predictive controllers (MPC) are a class of advanced process controllers that use a mathematical model of the actual plant or process to predict the outputs of the process in response to past controller actions. Figure 1 [1] shows an example of MPC response for a particular instant. These predictions are used as inputs to calculate the optimal future controller actions. The structure of MPC makes it superior to conventional PID controllers in terms of performance [1] and enables processes to operate close to variable constraints [2]. They are first utilized in the industry in the 1980s. The main motivation behind its development is its ability to handle processes with multiple inputs and multiple outputs in the presence of multiple constraints [3].

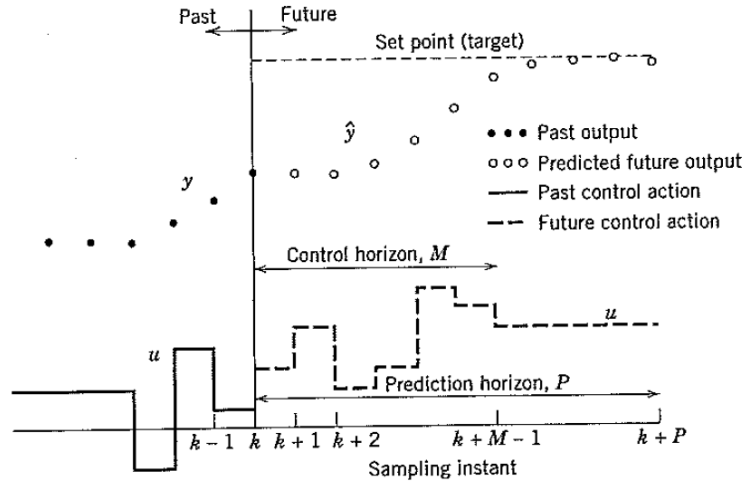


Figure 1: MPC response

As it is, the performance of MPC highly depends on the accuracy of the mathematical model employed. Over time, the difference between the incorporated model and the actual process will increase, affecting the performance of MPC. Some cases even led to shutdowns [3]. The phenomena is named model-plant mismatch. This is due to plant process changes brought about by the change in equipments, operating conditions, fouling or degradation [4]. Thus, it is essential for control engineers to have in depth knowledge on the relationship between the scale of MPM and the MPC performance. This will enable engineers to make decisions on whether corrective action is needed in the event of MPM. Furthermore, there is also a need for techniques to identify and isolate parts (sub models) of the model of the whole plant that contain MPM. This is because model re-identification requires intrusive tests on the plant equipment [2], causing the process of re-identifying the model for the whole plant time consuming and costly.

Responding to current needs, a mismatch estimation, detection and isolation algorithm is developed based on MPM modeling techniques such as autoregressive model average model with exogenous inputs (ARX) using MATLAB Simulink. The algorithm models the mismatch using model residual data, predict the mismatch using the mismatch model, compare the values with a significance threshold and finally decide on the presence of MPM. The algorithm analyzes all sub channels of the model to isolate the mismatch. This project will support this algorithm by

providing the thresholds of significant mismatch, generated from a stimulation using the available model.

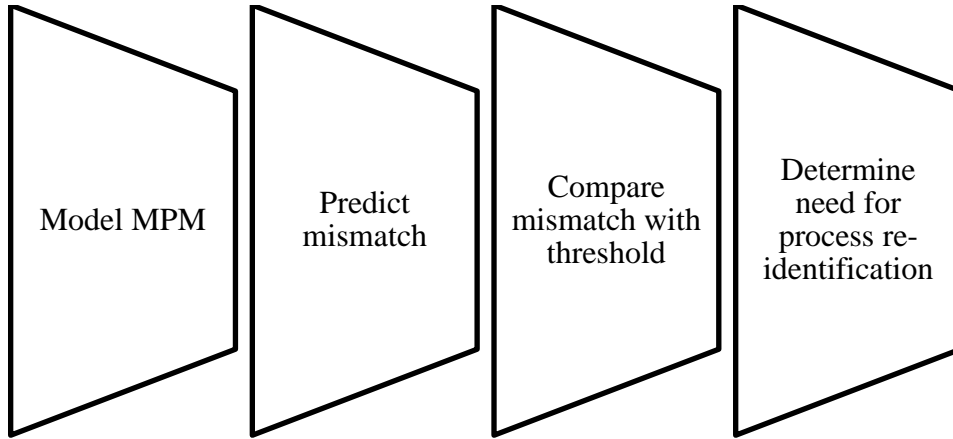


Figure 2: New MPM detection and isolation algorithm

## **1.2 Problem Statement**

There are limited research done that quantitatively measure the effects of MPM on the performance of MPC. This is particularly true in terms of comparative study between the scale of mismatch to the scale of impact on controller performance. This relationship is critical for control engineers to make informed decisions regarding the need for action to be taken in response to the presence of MPM. The study will also help develop a suitable method to determine the threshold of significant mismatch to be used as a benchmark in mismatch detection algorithms. Algorithms with built in consideration for mismatch significance in relation to its impact to performance gives critical information for re-identification decisions.

A model-plant mismatch detection algorithm is developed based on predictions of the parametric mismatch by a mismatch model. There is thus a need to compare the mismatch estimated with a predetermined threshold in order to make a decision on its significance.

## **1.3 Objectives**

- 1.3.1 To investigate the effects of model-plant mismatch on the performance of model predictive a controller.
- 1.3.2 To develop a method to determine the mismatch threshold.

## 1.4 Scope of Study

This study focuses on the relationship between MPM and MPC performance and how that relationship can be used to determine the threshold of significant mismatch in a newly developed MPM detection and isolation algorithm. The study is not concerned with the comparison between the performance of MPC and normal PID controllers.

The scope of MPC performance degradation factor is limited to model-plant mismatch in multiple inputs multiple outputs systems only. A two by two Wood and Berry distillation model is chosen here. The relationship between the magnitude of model-plant mismatch, specifically parametric mismatch in the gain, time constant and time delay, with the resulting control performance will be studied. Structural mismatch is not considered whereby a first order with time delay transfer function that is similar to the model structure is assumed to be sufficient to express the mismatch. In terms of performance, this study will utilize Integral of Absolute Error (IAE), Integral of Squared Error (ISE) and Integral of Time multiplied by Absolute Error (ITAE).

Only linear MPCs are utilized in this study, the scope does not include non-linear MPCs, nor does it include the comparison between linear and non-linear MPCs. This study will use a Wood and Berry model for a dual input and dual output distillation column as a benchmark for simulation studies.

The MPM detection and isolation technique mentioned in this study is a newly developed method that calculates and measures parametric mismatch. The mismatch is compared to a benchmark to determine which sub models contain mismatch. It uses a mismatch model to determine a closed loop mismatch measure.

### **Out of scope:**

- Non-linear MPC
- Comparison with PID controllers
- Effectiveness of other MPM detection and isolation techniques
- Other plant models

## CHAPTER 2

### LITERATURE REVIEW

#### 2.1 Model Predictive Control (MPC)

Model Predictive Control (MPC) is an advanced process control system that uses an approximated mathematical model of the process to predict the future outputs of the process in response to the inputs or manipulated variables. These predicted values are considered alongside the current process outputs to generate a series of ideal control steps that would bring the output of the process towards the set points in the most efficient manner, which in turn are calculated by maximizing or minimizing an economic objective function. The prediction model is usually developed in the state space, which can be expressed in a linear discrete time model as shown below in equation (1) [1].

$$\hat{y}(k + 1) = \sum_{i=1}^{N-1} S_i \Delta u(k - i + 1) + S_N u(k - N + 1) \quad (1)$$

Where  $\hat{y}(k + 1)$  is the output variable at  $k+1$  sampling instant while  $\Delta u(k - i + 1)$  denotes the change in controller output from one instant to the next and  $S$  denotes the step response coefficients.

A simplified model-based control structure can be seen below [5]:

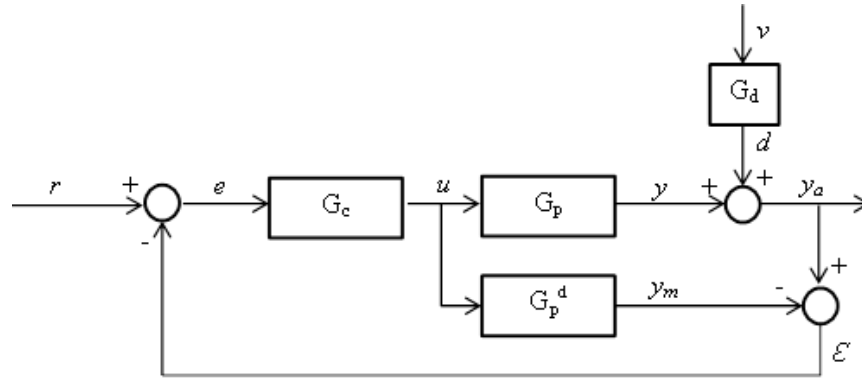


Figure 3: MPC Control Flow

Where  $G_c$ ,  $G_p$  and  $G_p^d$  represents the controller, process, and model transfer functions respectively.  $r$ ,  $e$ ,  $u$ ,  $y$ ,  $y_m$ ,  $v$ ,  $d$ ,  $y_a$ , and  $\mathcal{E}$  represents the set point, error, controller output, process output, predicted process output, disturbance input, disturbance output, actual process output and loop residuals respectively.

The other popular alternative in advanced process control is advanced regulatory control (ARC). MPC is now growing in terms of number and is almost caught up with ARC. It is slowly introduced in food processing and automotive manufacturing. Furthermore, larger companies are also found to be prone to consider MPC [6].

MPC is mainly developed to tackle control problems with multiple inputs and multiple outputs (MIMO) in petrochemical plants and oil refineries, where 60% of the total application of MPC in the industry resides. PID controllers are better at handling process disturbances when the controller gain and derivative term is big in a single input and single output (SISO) system. In MIMO systems where there are more than one set point and involves various process and control constraints, MPC will provide a simpler solution. This is because using PID controllers in these kinds of situations will require Shinskey type expertise in the dynamic decoupling of PID controllers. The required skills are now gradually diminishing [6]. Significant energy savings, product quality improvements and operating costs are brought about by MPC [2].

The effectiveness of MPC depends highly on the accuracy of the process model implemented throughout the life of the plant [1]. Model predictive control will deteriorate with time, some deterioration even led to shutdowns. Thus,

performance monitoring and deterioration diagnosis is essential successful implementations [3].

## 2.2 Model Predictive Control Performance

The main problems reported by Bialkowski and Kozub and Garcia for control loop performance deterioration is inadequate tuning, poor maintenance of hardware, control valve stiction, model-plant mismatch and stochastic disturbances [7]. A comprehensive approach to control performance assessments include determining current performance using measures such as output variances, selection and determination of a benchmark, detecting and diagnosing poor performance and lastly improvement of controller inputs [8]. More traditional performance measures are rise time, settling time, overshoot, offset and integral error [8]. These measures are deterministic and used by Jämsä-Jounela et al in their study of the control of a floatation cells in a zinc plant [9].

One of the first researches done on MPC performance monitoring is by Harris, where the lower bound of achievable controlled variable variance is derived from an equivalent multivariable control system and used as a benchmark. This minimum variance control is calculated from routine process data [10]. The Harris index introduced also includes variance measures of the manipulated variable. Using routine operational data, Huang and Shah developed a method that seeks a suitable explicit expression of the feedback controller-invariant term for the closed-loop multiple inputs and multiple outputs process. This term is subsequently used a benchmark for performance [11].

$$\eta_{\text{HARRIS}} = \frac{\sigma_{MV}^2}{\sigma_y^2} \quad (2)$$

Schäfer and Cinar proposed a benchmark that takes the ratio of the historical and actual performance. The performance measure used is the variance of the control error and the control moves [4].

For advanced measures, Grimble suggested a generalized minimum variance, which is the extension of the Harris index taking into account control action penalty. Huang and Shah proposed the linear-quadratic Gaussian (LQG) benchmark [8].

$$J_{LQG} = var\{y(k)\} + \lambda var\{\Delta u(k)\} \quad (3)$$

Reviewing the literature, it is determined that deterministic measures are the most suitable to be utilized in this project as it enables direct correlation between the performance and MPM in order to find the threshold of significance. Deterministic measures can also be applied to more specific sub units. On the other hand, stochastic measures deal with the performance of the plant in general.

The table below summarizes the findings:

Table 1: Summary of literature for controller performance measurement

Author	Summary
(Harris 1989)	Stochastic measure: Minimum variance approach
(Harris, Boudreau et al. 1996)	Expanded minimum variance approach to MIMO systems, highlighted interaction effects
(Huang, Shah et al. 1997)	Stochastic measure: Feedback controller invariant term based on FCOR analysis
(Jämsä-Jounela, Poikonen et al. 2003)	Studied the use of deterministic measures such as PE, IAE, ISE, ITAE and ISU.
(Schäfer and Cinar 2004)	Stochastic approach: Ratio between historical and actual performance
(Jelali 2006)	Developed a comprehensive approach to control performance assessment.
(Huang and Shah 1999) in (Jelali 2006)	Stochastic approach: Linear-Quadratic Gaussian benchmark
(Grimble 2002) in (Jelali 2006)	Stochastic measure: Generalized variance measure

### 2.3 Model-Plant Mismatch (MPM)

Controllers are subjected to all kinds of errors. Errors that may incur during the design stage include approximations of the prediction and disturbance model and assumptions on the operating conditions. Controllers that perform well at the start still may be subjected to errors thereafter. The performance of controllers will deteriorate over time due to sensor or actuator failure, equipment fouling, variation

in feedstock and product specifications and seasonal influences. Up to 60% of all industrial controllers fall prey to performance degradation [4].

For MPC systems, one of the main issues is model-plant mismatch. Model plant mismatch is one of the main factors for poor control loop performance [7]. This is where the model used by the controller is unable to accurately predict the outputs of the process due to physical changes to the plant such as equipment fouling, changes in parts of the plant and product specification change leading to changes in operating conditions. These conditions lead to a difference in the mathematical model identified during design that is implemented in the controller and the current actual model of the plant.

A linearized and simplified mathematical model of the process is usually employed in MPC. As such, there will be naturally a mismatch between the proposed model and the actual process due to high nonlinearities and high order dynamics of actual processes. However, a feedback system integrated in the controller will be able to deal with small mismatches, resulting in many successful implementations of the simplified models in the industry. As the mismatch increases due to the aforementioned factors, the controller performance might degrade to a degree where product quality and system stability is compromised [5].

#### **2.4 Detection and Isolation of Model-Plant Mismatch**

Various researches have sought to develop algorithms and methods to detect and isolate model-plant mismatch. These techniques can be classified based on methods of mismatch measure and analysis methods [5]. It should be noted that the techniques reviewed here are ones that are applicable to MIMO systems only. Parametric mismatch assumes that the mismatch can be measured by the additive or subtractive deviation in gain, time constants and delay constants of the model transfer functions. They are a subset of transfer function based measures. The advantage is easy relations to physical parameters, this relation would enable engineers to isolate the part of the plant mismatched by matching the transfer function parameters that deviated with its corresponding physical variables. When

the mismatch is in the structure of the transfer function itself, it is categorized as structural mismatch [5].

Wang et al. proposed a method to detect parametric mismatch and isolation by using routine closed loop operational data. The method models the process using Markov parameters and the Subspace approach and can accurately detect parametric mismatches in plant models [12, 13]. Selvanathan and Tangirala proposed a method for parametric mismatch detection by introducing a new quantity: plant model ratio  $G_p/G_m$  which is also estimated from routine closed loop operational data [7]. This structure is noted to have potential to measure structural mismatch [5]. Their studies show that there is a unique signature in the plant model ratio for each type of parametric mismatch. Their method is developed using frequency response functions of the plant and model transfer functions [7]. The plant model ratio measure is further investigated by Kaw et al. In their study, they improved the methodology of MPM detection and isolation by introducing an assessment procedure made up of statistical procedures to minimize estimation effort in terms of number of unknowns and an optimal set-point design for the plant model ratio method. They found that the method can only be used to detect deviations in gain, dynamics and delay but not between time constants. Their work reduced the minimal excitation to only 2 frequencies [14].

$$\Delta_{PMR} = \frac{G_p^m(s)}{G_p^d(s)} \quad (4)$$

Using routine closed loop operational data, Badwe et al. also formulated an algorithm to detect and quantify the impact of MPM. Three sensitivities are proposed as measure: relative sensitivity (ratio between actual to design error), designed sensitivity and the variability ratio. In addition, their studies found that the direction of the set point dithering signal also affects the measure of MPM [15].

Other transfer function based measures include the Vinnicombe metric, which utilizes the left and right normalized co-prime factorizations [16] and the generalized closed-loop error transfer function [17]. These measures however, have not yet been studied in the context of MPM detection and isolation.

Jiang et al. formulated the MPM detection and isolation problem in the discrete time state space measure. They proposed 3 MPM detection indices for the detection of MPM and also a logic methodology to isolate the state space parameters of mismatch. The approach is driven by data and is parametric in nature. The process however, can only isolate the state space matrix that has mismatch and not the individual components of gain, time constant and time delay [18]. Wang et al.'s method is similar, where Markov parameters are utilized. Markov parameters are derived from the discrete time state space measure by setting the inputs to impulse signals [5].

A variable based measure identifies the presence of correlation between the model residuals and the inputs. This correlation will point towards model plant mismatch when the noise is white in an open loop system [5]. Badwe et al. proposed a technique to detect model-plant mismatch by the analysis of partial correlations between model residuals and the manipulated variables in closed loop, colored noise systems as shown in equation (5). This technique filters out the effect of disturbances in the model residuals so that mismatch can be accurately detected from the routine operation data [19].

$$\varepsilon = \Delta_{add}u + G_d d \quad (5)$$

To solve the linearity problem that stems from autocorrelation and cross-correlation between input variables in MIMO control, Kano et al. proposed a statistical stepwise variable selection method to determine sub models that contain significant mismatch. A sub model is concluded to have model plant mismatch when a large enough number of past inputs is determined to contribute to the correlation. Routine process data is utilized [20]. Webber and Gupta introduced a technique that checks for correlation between the set-point that is manipulated to become a dithering signal to the model residuals. The dithering is introduced to overcome problems of colored noise affecting the correlation between  $u$  and the set point. They also used the cross correlation approach to determine the sub models that contain the mismatch [21].

Ji et al. uses a three point frequency response estimation to test an online system. The results are used to quantify the errors in a model error index matrix by

comparing it with the frequency response of the current model, taking into account an upper error bound [22].

Earlier in time, researchers mainly focused on detecting the mismatch and not isolating them. These techniques are also known as model validation techniques. Kesavan and Lee proposed a statistical chi-squared test to determine MPM. The test is done on the errors of output and prediction with operational data [23]. Huang formulated a model validation detection algorithm using two-model divergence algorithm in the frequency domain [24]. Kammer et al. in turn developed a semi-intrusive MIMO model invalidation technique by analyzing the deviation between open-loop and closed-loop signals. The technique enables a disturbance model to be identified during open loop. This model is then compared with the model of white noise. If there are no differences, MPM is not present [25]. Kendra and Cinar studied a method that uses sensitivity functions of a MIMO system in the frequency domain. The results are compared with the design specifications, a mismatch will be detected if it differs from the design [26]. Harrison and Qin devised a method to differentiate between MPM and disturbance on the poor performance of MPC. The method monitors the innovations of the Kalman filter to look for autocorrelation. The order of the correlation will determine if either MPM or noise is causing the suboptimal operation of the controller [27].

Mismatch identification techniques can also be categorized as partial or holistic mismatch. Partial mismatch detects mismatch in the sub model elements while holistic mismatch detects mismatch in the whole matrix. Both partial and holistic mismatch is considered in Badwe et al. and Kano et al. [5]. Open loop mismatch parameters are mostly studied in the above research papers. They include deviations in gain, time constants, delay time, state space parameters, additive and multiplicative deviation of transfer functions and the plant model ratio. They take into account the changes caused by the process itself only. Closed loop parameters such as the  $v$ -gap (Vinnicombe metric) and generalized close loop error transfer function are better at identifying mismatches in closed loop as there is sometimes a large difference in the response of closed loop dynamics when compared to open loop dynamics in response to a mismatch [5]. Closed loop techniques are also better at capturing control relevant frequencies in the data generated, enabling the corrective action to better suit closed loop performance specifications [15]. Finally,

there is a distinction between direct and indirect mismatch detection techniques. Direct techniques use mathematical models such as ODEs, transfer functions, state space equations or Markov parameters. Indirect techniques use correlations or explanatory relationships, such as in Kano et al. and Badwe et al. [5].

Reviewing these techniques, the following critical analyses are developed:

- Model-plant mismatch detection and isolation techniques are mostly developed separately from MPC performance studies. The newly developed method is advantageous as it will give indications on the scale of mismatch to be used to determine the significance of the MPM detected.

The findings are summarized in the table below:

Table 2: Transfer function based techniques

Author	Summary
(Jiang, Li et al. 2007)	Measure mismatch using model deviation indices in discrete time space
(Badwe, Patwardhan et al. 2010)	Measure MPM using relative sensitivity, designed sensitivity and the variability ratio
(Selvanathan and Tangirala 2010)	Plant model ratio using the frequency response of both the plant and model
(Wang, Xie et al. 2012)	Review of MPM measures
(Wang, Song et al. 2012)	Utilize Markov parameters for mismatch measure, similar to the discrete time space approach
(Kaw, Tangirala et al. 2014)	Further developed plant model ratio, introduced optimal set point design method of only 2 frequencies
(Vinnicombe 2000) in (Wang, Xie et al. 2012)	Measure MPM using the v-gap metric (not studied in terms of mismatch detection)
(Wan and Huang 2002) in (Wang, Xie et al. 2012)	Closed-loop error transfer function (not studied in terms of mismatch detection)

Table 3: Variable based and model based validation techniques

Author	Summary
(Webber and Gupta 2008)	Correlation between a dithering signal and model residuals, use cross-correlation to isolate sub models
(Badwe, Gudi et al. 2009)	Partial correlation between model residuals and controller action
(Kano, Shigi et al. 2010)	Proposed stepwise statistical variable selection method for isolate sub models with mismatch
(Ji, Zhang et al. 2012)	Compares frequency responses of real process and model

	to detect and isolate mismatch
(Kesavan and Lee 1997)	Model validation technique: Statistical chi-squared method between output errors and operational data
(Kendra and Cinar 1997)	Model validation technique: Sensitivity functions
(Huang 2001)	Model validation technique: Two-model divergence algorithm in the frequency domain
(C. Kammer, Gorinevsky et al. 2003)	Model validation technique: Developing disturbance model and comparing it to white noise
(Harrison and Qin 2009)	Differentiate between MPM and disturbance by monitoring the Kalman filter to determine the order of autocorrelation

## 2.5 Quantifying the Impact of MPC on MPM Performance

Most of the current research literature measure MPC performance based on the MPM measures developed, as mentioned in the subtopic 2.4. They correlate the deviation of model parameters with the magnitude of MPM measure (which is formulated) that is produced. There is however, a lack research on the effect of model parameter deviation on the change in MPC performance measured based on elements of the objective function. These measures such as Integral absolute error (IAE), Integral squared error (ISE), Integral time multiplied by absolute error (ITAE), input variation and robustness. The relationship is important as it directly shows to what extend and scale MPM affects the controlled variables like product composition or quality.

## 2.6 Process Re-identification

MPM can be corrected by process re-identification. Process re-identification involves intrusive tests on individual plant equipment or unit operations in order to determine the new plant model, assuming that the model has changed due to physical changes in the plant. Any part of the plant which model has to be re-identified has to be stopped and isolated for experiments. A full plant process re-identification is expensive, time-consuming and causes production interruption for several weeks, resulting in huge losses. Therefore, for MPC controllers, deterioration in controller

performance needs to be supported with more information or studies before a process re-identification is done. This is because the performance deterioration of MPC may be caused by sustained disturbances or unknown feed variations, which may be mistaken as MPM. If this happens, re-identification will be redundant [2].

Detection of MPM accurately is thus critical. There is also a need to quantify the extend of impact MPM has on MPC performance and isolate parts of the plant that has MPM. This is because MPC performance deterioration is usually due to mismatch in only parts of the plant [12]. This would provide the necessary information to make decisions regarding the need for performance correcting efforts like process re-identification. Isolating MPM to parts of the plant would also prevent the need to shut down the whole plant to carry out process re-identification on every plant unit, which will then significantly cut cost and operational down time.

Conner and Seborg put forward a procedure that introduces a simple test for closed loop data in order to determine model validity. They propose a “simple test” using statistical methods such as PCA (Principle Components Analysis) similarity factor and  $\Delta AIC$  (Akaike Information Criterion) statistic. Faults found with these metrics readily points towards changes in the actual process model [2].

Olivier and Craig proposed a data driven method to derive a MPM representative transfer functions from routine operational data. The technique has the potential to enable the results to be utilized in the controller without the need for process re-identification. The method however, requires accurate data with known disturbance models [28].

## CHAPTER 3

### METHODOLOGY

#### 3.1 Tools and Software

Table 4: Tools and software

Mathematical Process Model	2×2 I/O Distillation Column by Wood and Berry [29]
Software	MATLAB-Simulink

***Wood and Berry Mathematical Process Model:***

$$\begin{bmatrix} X_D(s) \\ X_B(s) \end{bmatrix} = \begin{bmatrix} \frac{12.8e^{-s}}{16.7s + 1} & \frac{-18.9e^{-3s}}{21s + 1} \\ \frac{6.6e^{-7s}}{10.9s + 1} & \frac{-19.4e^{-3s}}{14.4s + 1} \end{bmatrix} \begin{bmatrix} R(s) \\ S(s) \end{bmatrix} + \begin{bmatrix} \frac{3.8e^{-8.1s}}{14.9s + 1} \\ \frac{4.9e^{-3.4s}}{13.2s + 1} \end{bmatrix} F(s) \quad (6)$$

Equation (6) represents the distillation mathematical model by Wood and Berry [29].  $X_D$  and  $X_B$  refer to the distillate and bottoms composition while  $R$ ,  $S$  and  $F$  refer to the reflux flow rate, steam flow rate and feed flow rate respectively.  $R$  and  $S$  are the manipulated variables while  $F$  is the disturbance variable. For this project, the measure disturbance  $F(s)$  is set to 0 to prevent it from affecting the plant performance. This will ensure any effects are due to MPM only.

In terms of the phrases used in the results, Gain11, Tau11 and Delay11 will refer to the parameters in the first transfer function and so forth for the other transfer functions. In this case the Gain11 values correspond to 12.8 from equation 6.

## 3.2 Description of Methodology

### 3.2.1 Single Parameter mismatch

The steps arranged in a flow chart in figure 4. First, a closed loop control simulation model is built in MATLAB-Simulink containing the process inputs, a model predictive controller, process model, predictive model and process outputs. Then, a matrix of model-plant mismatches is determined based on positive or negative deviations of transfer functions parameters on all sub models of the model. Applying these deviations to the simulation model, the closed loop response data of the process is generated and analyzed. Performance measures such as Integral absolute error (IAE), Integral squared error (ISE) and Integral time multiplied by absolute error (ITAE) is calculated. These values are then analyzed in conjunction with the MPM applied by plotting the performance measure against mismatch graph to study the correlation between them. Lastly, the thresholds are determined based on previous analysis.

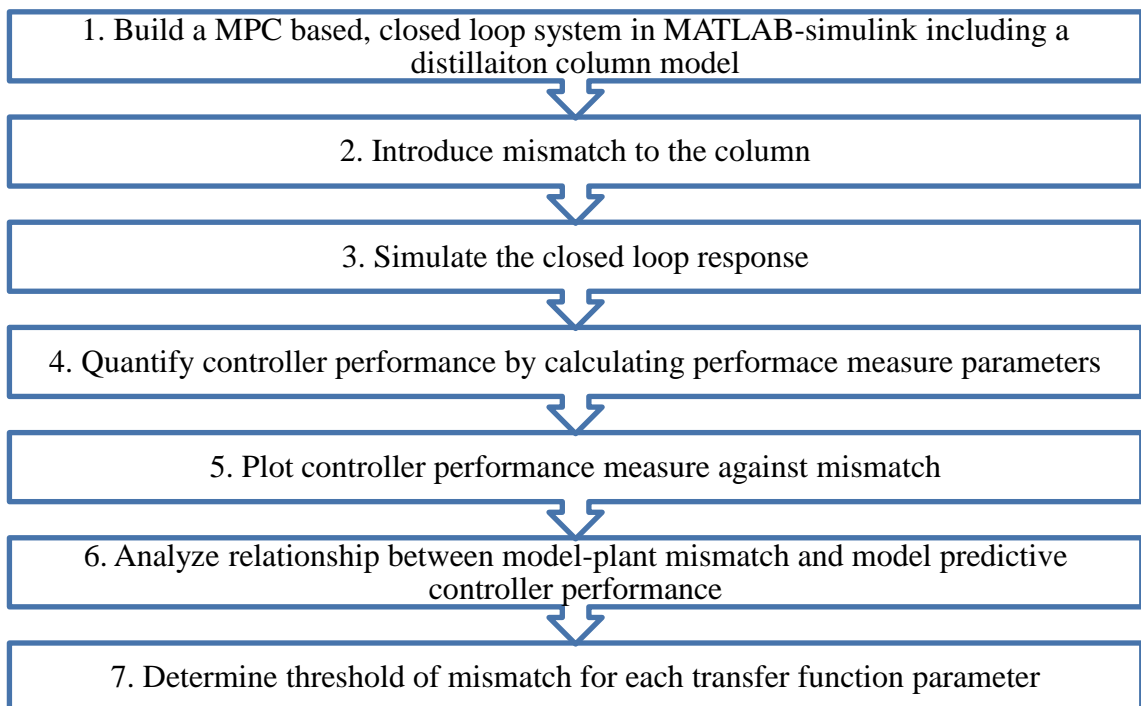


Figure 4: Process Flow

#### Step 1: Simulink model design

Figure 5 shows the Simulink model block flow diagram design. Model plant mismatch will be introduced by changing the parameters in the plant, as that will

signify physical changes. Due to the difference in models, the outputs  $X_D$  and  $X_B$  will differ from that of the model. There will thus be a difference  $e$  that can be simulated by taking the difference in signals. Values of  $e$  will then be used to calculate the performance measure and tabulated.

White noise is added to the plant output to simulate measurement noise. A disturbance model will also be fed to the model according to the Wood and Berry model. The inputs will be simulated with a dithering signal. Figure 11 shows the block diagram in Simulink.

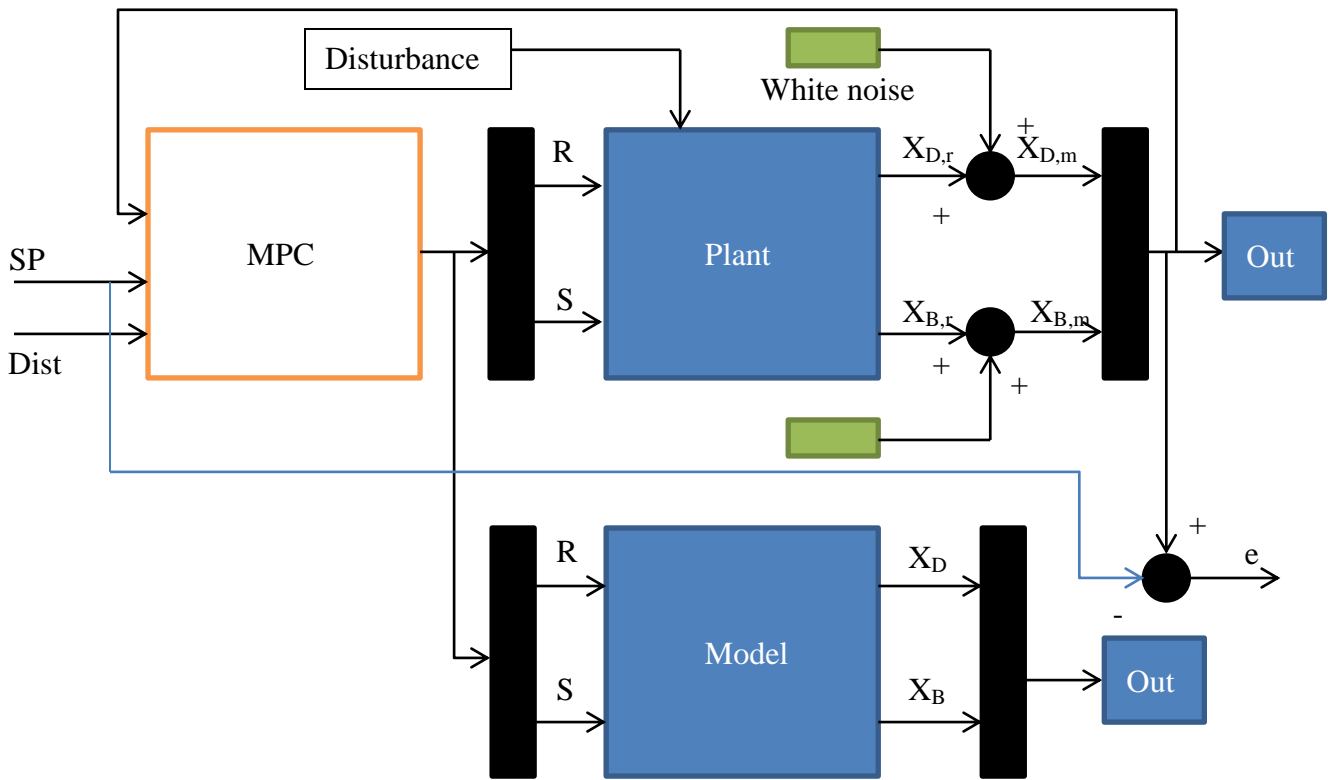


Figure 5: Simulink model block flow diagram

### Step 1a: Simulation settings

These settings are optimized based on the plant response to a step change in input at 0% mismatch.

Table 5: Simulation settings

Simulation time	100
Solver Step size	Variable step
Solver	ode45
Relative tolerance	1E-03
Input Step size	1
Input Step time	10
MPC control interval	1
Prediction horizon	100
Control horizon	10
Constraints	None
Overall weight tuning (robust to speed)	0.8
Input rate weight	0.1
Output weight	1
Overall estimator gain	0.5
Measurement noise	White (Magnitude = 1E-05)

### Step 2: Introduce mismatch

Model with MPM structure:

$$G_{p(mismatch)} = \frac{(K + \Delta K)}{(\tau + \Delta\tau)s + 1} e^{-(\theta + \Delta\theta)s} \quad (7)$$

Equation (7) shows the representation of the distillation column after mismatch has been introduced.  $\Delta K$ ,  $\Delta\tau$  and  $\Delta\theta$  will represent the deviation of gain, time constant and time delay of the column to the controller model respectively. Parametric mismatch are used in this study. The mismatch values are set based on percentages, where the range of percentages used is -40% to +40%, with a step size of 5%. The table below shows an example of the corresponding model parameters after application of mismatch.

Table 6: Sample of mismatch matrix

Mismatch	$\Delta K_{11}$	$K_{11,plant}$
-40%	-40%(12.8)	12.8-40%(12.8)
-20%	-20%(12.8)	12.8-20%(12.8)
0%	0	12.8
+20%	+20%(12.8)	12.8+20%(12.8)
+40%	+40%(12.8)	12.8+40%(12.8)

#### Step 4: Calculating performance measures

The performance of the plant is calculated based on deterministic measures, where the difference between the response and the intended output is quantified.

Deterministic performance measures are used in this study, the formulas can be referenced from Jämsä-Jounela et. al. [9].

- Integral absolute error:

$$IAE_i = \int_0^{t_i} |y_{pv}(t) - y_{sp}(t)| dt \quad (8)$$

- Integral squared error:

$$ISE_i = \int_0^{t_i} |y_{pv}(t) - y_{sp}(t)|^2 dt \quad (9)$$

- Integral time weighted absolute error:

$$ITAE_i = \int_0^{t_i} t |y_{pv}(t) - y_{sp}(t)| dt \quad (10)$$

These performance measures give different results in different situations. For example, when compare to IAE, ISE would magnify large errors in comparison to small errors. ITAE on the other hand, would give larger weightage to sustained errors. These differences are critical in this study in order to study all aspects of performance for MPC.

Each value of performance measure will correspond to a mismatch value, and thus a plot can be generated to observe the relationship.

#### Step 7: Determine the threshold of mismatch

After analysing the results for single parameter mismatch, it is determined that a percentage increase of the base IAE at 0% mismatch should be used as the criteria to determine the threshold of mismatch. An example can be seen below.

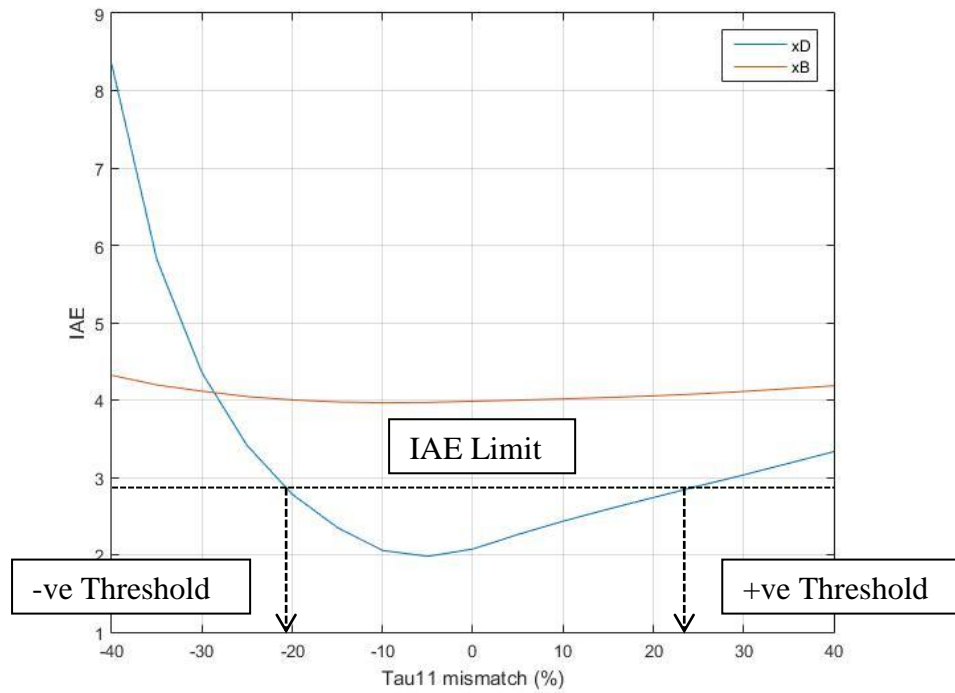


Figure 6: Threshold determination example

### 3.2.2 Double parameter mismatch

To study the interactions between different mismatch parameters on the plant performance when they are present at the same time, the steps from single parameter mismatch are repeated while varying two parameters at the same time. Surface plots are then generated from the IAE and the square vector of mismatches.

### 3.3 Key Milestones

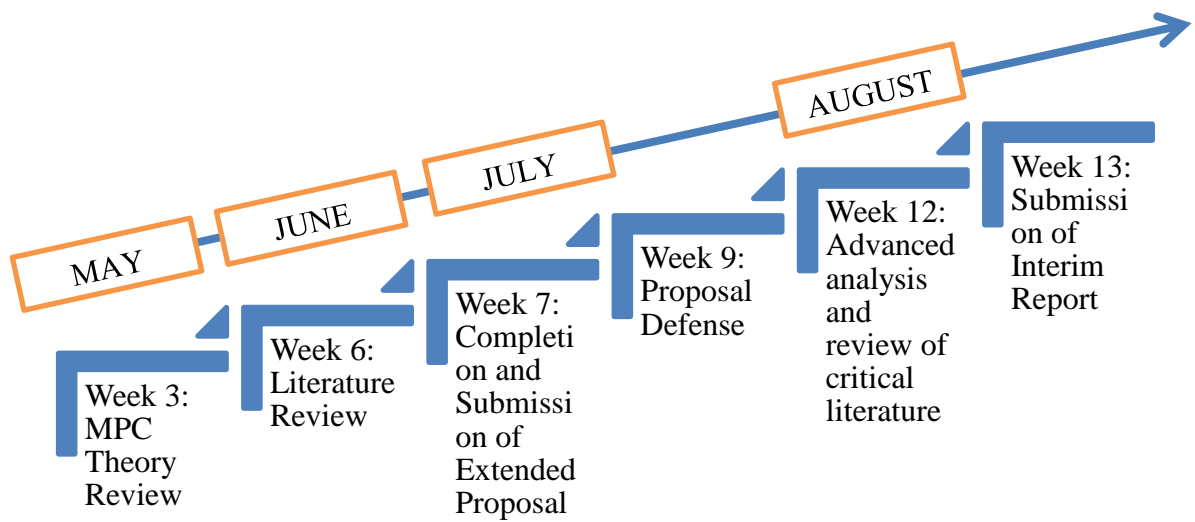


Figure 7: Key Milestones for May 2015 Semester

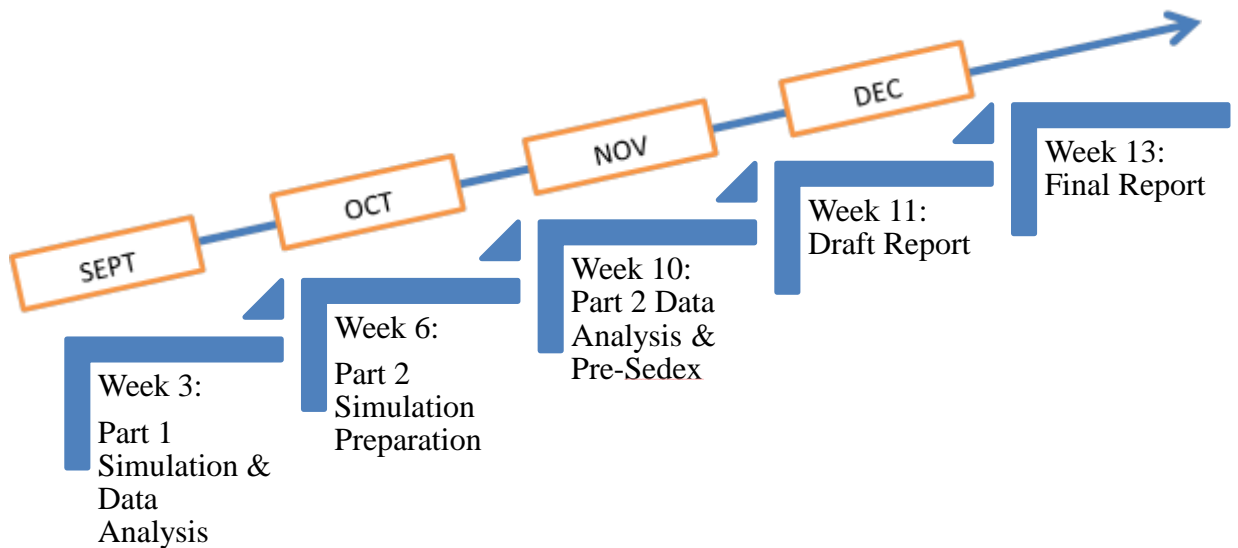


Figure 8: Key Milestones for September 2015 Semester

### 3.4 Gantt Chart

FYP I Gantt chart

Task	Week													
	1	2	3	4	5	6	7	8	9	10	11	12	13	14
Title Selection	■	■												
Collection of relevant literature			■	■	■									
Review of relevant MPC and MPM theory			■	■	■									
Review of literature			■	■	■									
Formulation of problem, objectives and methodology						■	■							
Preparation of extended proposal						■	■							
Proposal defense									■					
Advanced review and analysis of critical literature								■	■	■	■	■		
Make improvements to research methodology										■	■	■		
Study simulation techniques and detection algorithm											■	■	■	
Build simulation system for part 1												■	■	■
Preparation of the interim report												■	■	■
Submission of interim report												■	■	■

Figure 9: Gantt chart (FYP I)

FYP II Gantt chart

Task	Week													
	1	2	3	4	5	6	7	8	9	10	11	12	13	14
Part 1: Single variable mismatch simulation	■	■	■	■										
Part 1 results analysis				■	■									
Part 2: Double variable mismatch simulation					■	■	■							
Part 2 analysis							■	■	■					
Preparation of progress report						■	■							
Pre-sedex										■				
Preparation of dissertation								■	■	■	■	■		
Sedex													■	
VIVA													■	
Preparation of final dissertation													■	■

Figure 10: Gantt chart (FYP II)

## **CHAPTER 4**

### **RESULTS AND DISCUSSION**

#### **4.1 Single Parameter Mismatch**

##### **Analysis of IAE, ITAE and ISE**

There are three types of single parameter mismatch studied, the gain, time constant and time delay of the 1<sup>st</sup> order with time delay transfer functions. Figure 11 shows the IAE, ITAE and ISE for Gain11 mismatch while figure 12 shows the IAE, ITAE and ISE for Gain22. Deterministic measures such as IAE is more indicative of the plant performance during set point change excitation [9].

From figure 11 and figure 12, the shape of IAE and ITAE graphs are similar, despite the calculation of ITAE giving more weight to errors that occur later in time. This shows that the higher the absolute error (IAE), the longer the error sustains (ITAE). The IAE and ITAE will show different shapes only if similar IAE values correspond to different durations of sustained error. Since this trend is present throughout the entire study, the duration of sustained error can be inferred from the IAE.

Comparing ISE with ITAE and IAE, we see that the slopes of the ISE graphs are quite small. This shows that the size of error does not change much across the mismatch matrix. Thus, it is not a good measure to study the effect of model-plant mismatch. When there are significant differences of ISE between the positive and negative mismatch, such as in figure 12, the same trend is seen in IAE. Thus, the trend of ISE can also be inferred from the IAE since the larger the IAE, the higher the ISE. In physical terms, this can be explained by the higher the absolute error (IAE) corresponds to higher error sizes (ISE).

Therefore, IAE is chosen as the performance measure to analyze the effect of model-plant mismatch in this study as it can be used to infer both ITAE and ISE in addition to having clear slopes. The nature of the responses in this study show that a larger IAE will only correspond to larger error sizes and longer sustainment of the error. Figure 13 shows the output response for no mismatch, to be used for comparisons later.

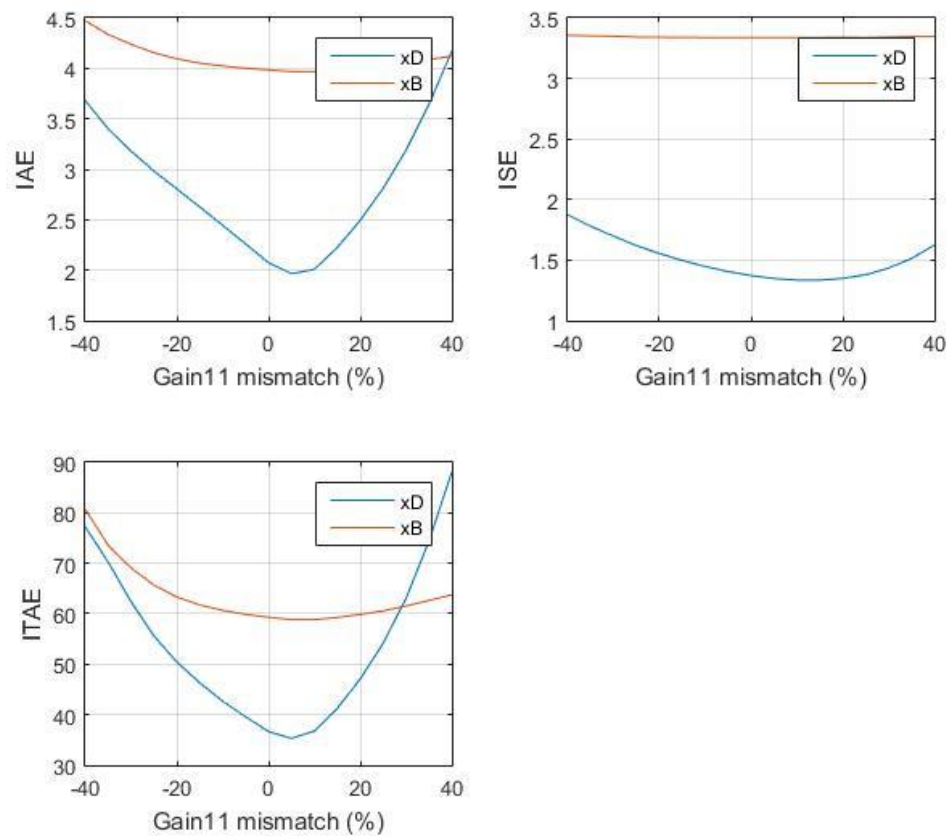


Figure 11: Gain11 mismatch IAE, ITAE and ISE

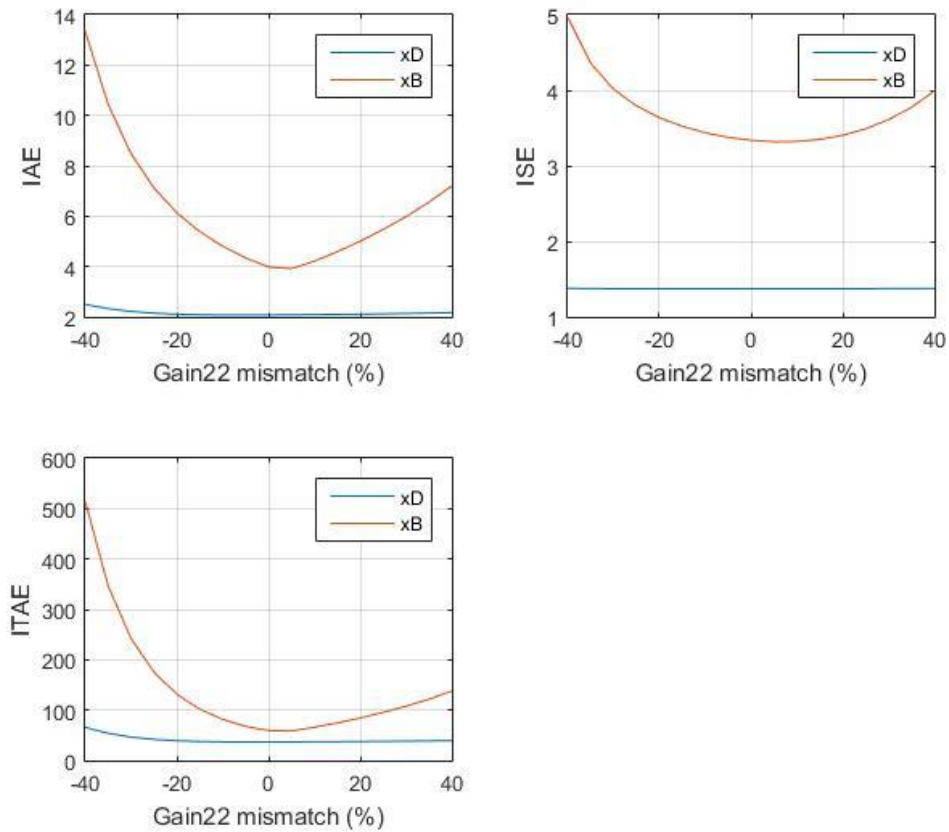


Figure 12: Gain22 mismatch IAE, ITAE and ISE.

### Common trends

There are two common trends that persist across the results for single gain, time constant and time delay mismatch. The first trend is that an increase in mismatch (regardless of sign) will generally always increase the IAE, ITAE and ISE. The results support the general consensus that increased MPM will deteriorate plant performance [30]. This cause the shape of the IAE graphs is V shaped, with the minimum at 0% mismatch and high values at the high mismatches. The only exceptions are during certain high time delay mismatches where the maximum IAE is not at the extreme mismatch percentages and during gain and time constant mismatches where very small mismatches sometimes have lower IAE than 0% mismatch. The reasons for these exceptions are explained in the relevant parts respectively.

The second trend is that the mismatch of parameters of a transfer function only significantly affects the output directly dependent on it, the other output is only affected when the IAE is very large. This effect however, is still minor compared to the effect on the mismatch on the main output. For example, a -40% mismatch in Gain11 only contributes to a +12% increase in IAE for  $x_B$ , when compared to a +77.5% increase in IAE for  $x_D$ . This trend can be seen in the relatively flat shapes of  $x_B$  in figure 11 and  $x_D$  in figure 12. Thus, for mismatches in transfer function 11 and transfer function 12, only the effect on  $x_D$  is observed while for mismatches in transfer function 21 and transfer function 22, only the effect on  $x_B$  is observed.

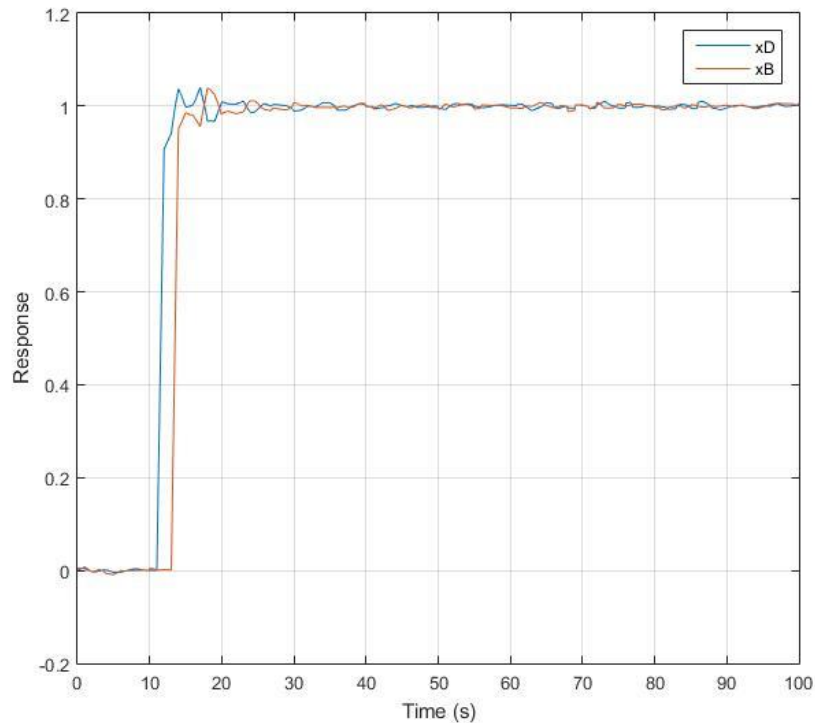


Figure 13: Plant response for 0% mismatch

#### 4.1.1 Single gain mismatch

The full results are included in the appendix. The relationship between the IAE and mismatch are approximately linear in nature for the outputs affected by the mismatch for Gain11 (Figure 11), Gain12 and Gain21. However, the result for Gain22 (Figure 12) shows a curved slope for negative percentage mismatch. The plant output responses for the relevant mismatches show that the responses contain

an offset that slowly reduces with time. Therefore, a curved slope is an indication of a semi-permanent offset while a near linear relation signifies that the system is still stable across the mismatch.

Comparing the overall  $x_D$  IAE between Gain11 with Gain12 and  $x_B$  IAE between Gain21 and Gain22, it is found that the higher the magnitude of the gain, the higher the effect of percentage mismatch on the plant performance. This is expected as a higher gain magnitude translates to a higher actual mismatch magnitude for a similar percentage mismatch.

There are in general only small differences in IAE between mismatches of opposite signs. The differences are can be linked to condition number trends as seen in figure 14 [1].

### **Condition number and plant controllability**

Contrary to the common trend, at small gain mismatches (<5%), the IAE of the overall system may improve from 0% mismatch. It is noted that the local minimum for the IAE are not at 0% gain mismatch. For Gain11 and Gain22, the minimum error occurs at +5% gain mismatch while for Gain12 and Gain21, the minimum error occurs at -5% gain mismatch. This can be seen in figure 11 and figure 12. This indicates that a slight gain change in the plant towards a certain direction makes the control performance of the plant better. The reason is that the plant becomes easier to control due to the changes in the plant, resulting in overall better plant performance despite the presence of mismatch. The results agree with the trend of condition numbers of the system as seen in figure 14. The local minimum will tend towards the direction of mismatch where there are smaller conditional numbers, indicating that the system becomes easier to control.

This phenomenon however, is not significant for gain mismatches higher than 5%, the negative effect of model residuals on the controller performance is much higher than any positive effect the mismatch may have on the controllability of the plant. The local minimum can however indicate the direction of decreasing condition number and show the direction of mismatch that makes the plant easier to control.

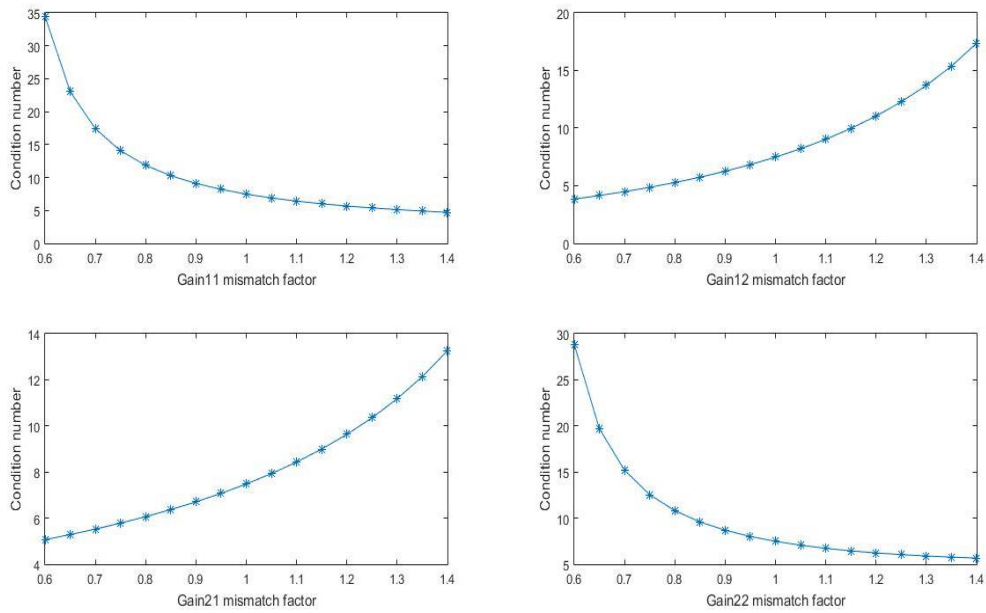


Figure 14: Condition numbers for gain mismatch

### Plant step response analysis

Figure 15 shows the plant response for a +40% Gain11 mismatch while figure 16 shows the plant response for a -40% Gain11 mismatch. Comparing the response of the plant output with figure 13 (no mismatch), it is found that the plant response becomes more oscillatory, vigorous; with higher overshoot when the percentage gain mismatch is positive. On the other hand, the plant response becomes more sluggish with less overshoot but have small sustained errors when the percentage gain mismatch is negative.

This is because a positive percentage gain mismatch will increase the magnitude of the plant gain and thus cause the plant output to be higher than the predicted output. Since the MPC constantly under predicts the magnitude of output change, the controller action would be more vigorous than needed. The reverse occurs during negative percentage gain mismatch, where the magnitude of the plant gain will decrease. The MPC constantly over predicts the magnitude of change, causing the controller action to be lower than needed, resulting in a sluggish response. The same trend is observed for Gain12, Gain21 and Gain22.

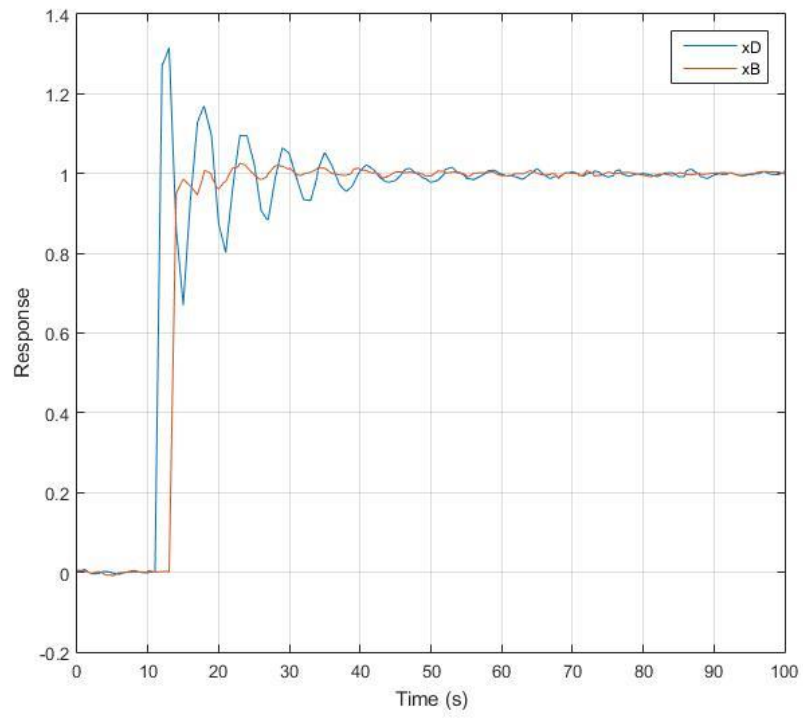


Figure 15: Plant response for +40% Gain11 mismatch

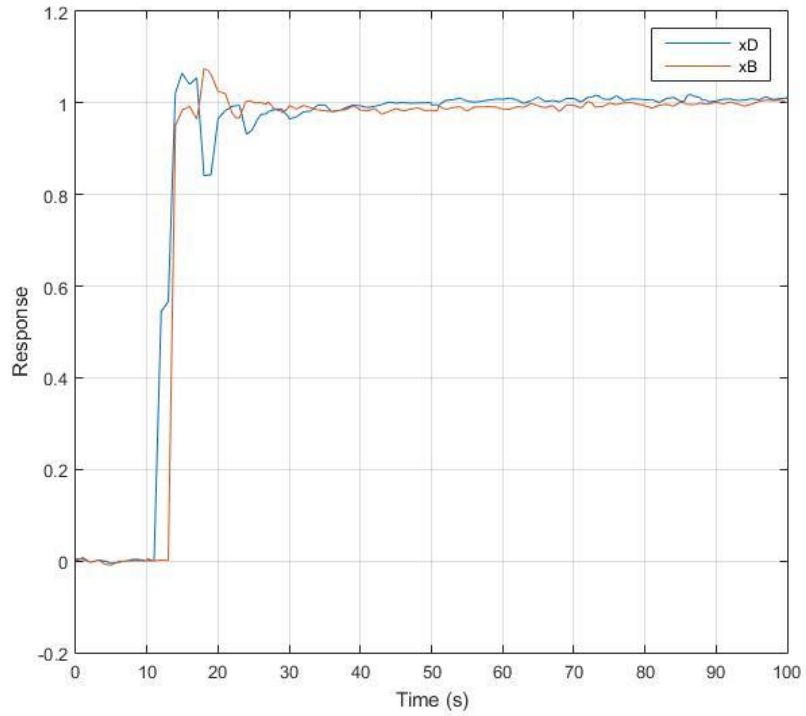


Figure 16: Plant response for -40% Gain11 mismatch

### 4.1.2 Single time constant mismatch

Figure 17 shows the overall IAE trend for Tau11. The overall IAE shape for all four time constants are similar and are included in the appendix.

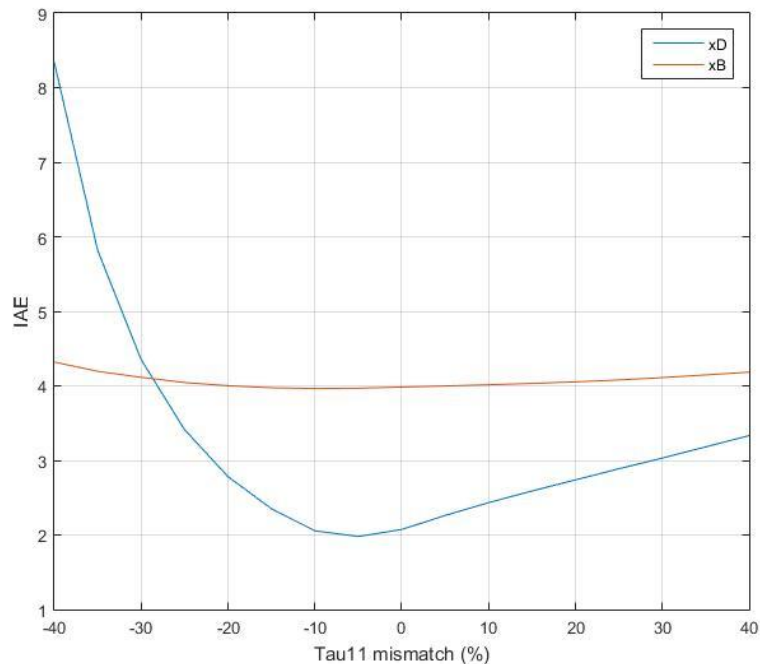


Figure 17: Tau11 mismatch IAE

There are significant differences between positive and negative percentage mismatch. The IAE slope for increasing positive mismatch is low and approximately linear. Increasing magnitude of negative mismatch however results in a much higher slope with a more exponential like curve, as seen in figure 17. This trend is consistent for all four time constants and would be further explained in the plant step response analysis part.

For time constant mismatch, there is no correlation between the original magnitudes of time constant with the magnitude of the resulting IAE, unlike gain. Tau11 has a higher impact compared to Tau12 while Tau22 has a higher impact compared to Tau21.

### **Plant controllability with small mismatch**

The local IAE minimums for all time constant IAE graphs are not at 0% mismatch but at  $\pm 5\%$ , which varies with each time constant. Tau11 and Tau22 have local minimums at -5% while Tau12 and Tau21 have local minimums at +5%. At first glance, it seems that this result does not support the plant controllability theory that systems with lower time constants are easier to control [31]. However, comparing it with the local minimums during gain mismatch, they are completely opposite for each transfer function. It can be then inferred that the local minimums may be dependent more on gain than time constant. When increasing the gain for a transfer function decreases the condition number, decreasing the time constant of that transfer function makes the plant easier to control. This is due to a faster attainment of the gain.

### **Plant step response analysis**

Figure 18 shows the step response for -40% Tau11 mismatch while figure 19 shows the response for +40% Tau11 mismatch. These figures can be compared with figure 3 (0% mismatch).

Comparing the responses, it can be seen that negative time constant mismatch cause a vigorous and oscillatory response with higher overshoot while positive time constant mismatch cause a more sluggish and slow response with lower overshoot. Taking into account the IAE trend from figure 17, it can be concluded that the higher IAE is due to a vigorous and oscillatory response. The sluggish response on the other hand, do not cause as much overshoot and stays within set point despite having the same magnitude of mismatch.

The responses can be explained by the nature of controller output in the presence of mismatch. Negative time constant mismatch makes the actual plant respond much faster than the controller predictions, thus, the controller is underestimating the response during transient conditions. The controller output will thus be more vigorous than needed and this will cause a vigorous response in the actual plant.

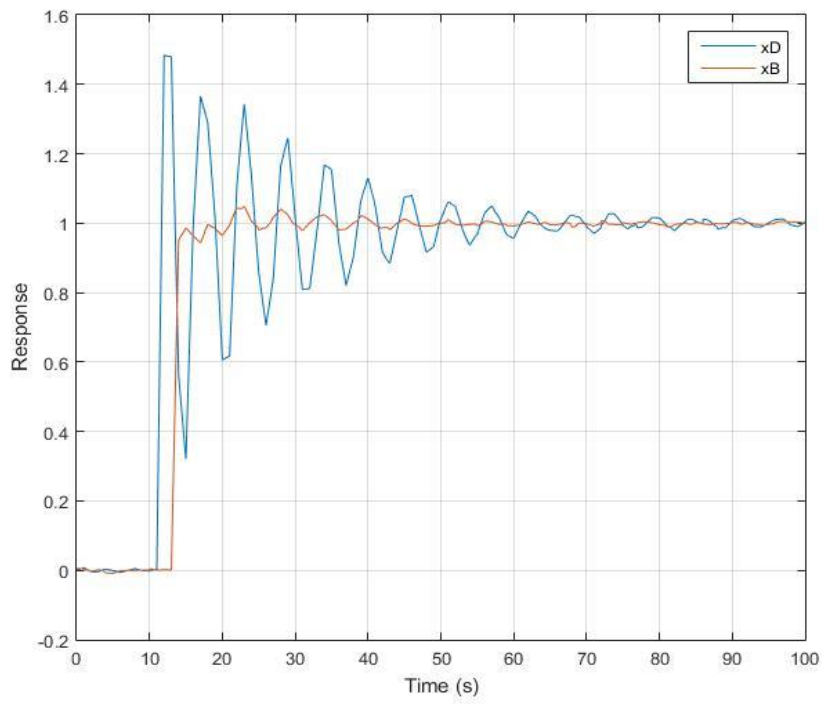


Figure 18: Plant response for -40% Tau11 mismatch

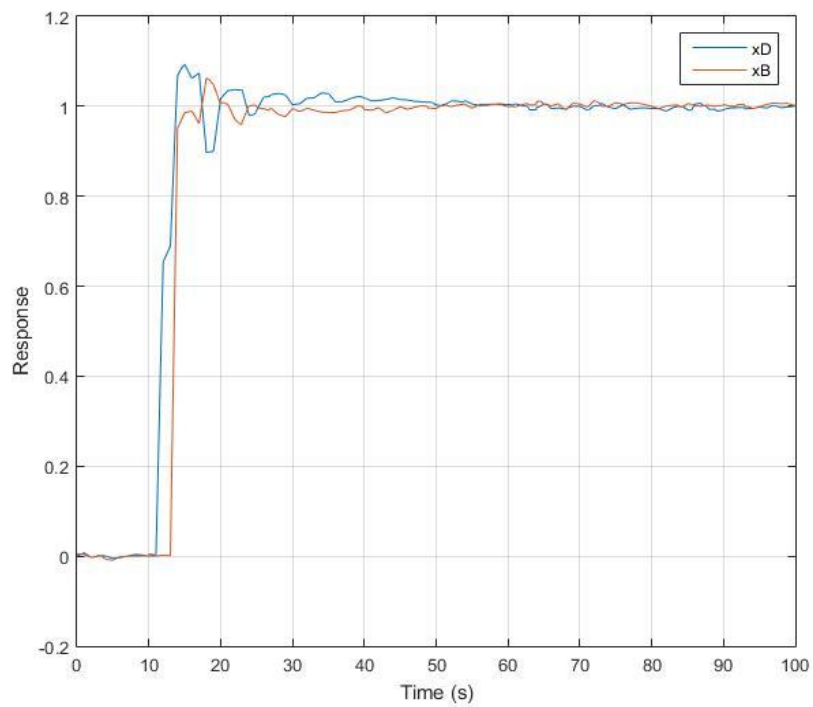


Figure 19: Plant response for +40% Tau11 mismatch

On the other hand, the controller overestimates the plant response in the presence of positive time constant mismatch during transient conditions. The plant responds more slowly compared to the model. The controller output would then be less vigorous than ideal and cause a sluggish response. However, the effect of mismatch is much less significant because response does not oscillate vigorously. These trends are consistent for all four transfer functions.

### 4.1.3 Single time delay mismatch

Figure 20 shows the overall IAE trend for Delay11. Compared to gain and time constant, the overall IAE shape for time delay is less smooth. This is due to severe instability that will be explained with the step response analysis. Time delay is also noted to affect the IAE more in general than time constant and gain.

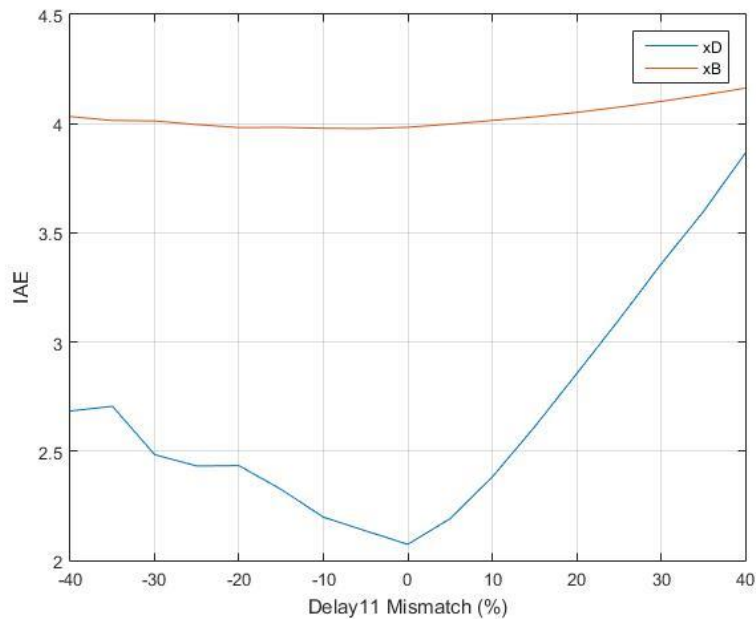


Figure 20: Delay11 mismatch IAE

There are significant differences between positive and negative percentage mismatch. Delay11 gives lower IAE for negative percentage mismatch while Delay12 and Delay22 gives lower IAE for positive percentage mismatch. Delay21

shows no significant differences. There seems to be no apparent inclination for these differences at the current mismatch range. This proves that due to interactions, an increase in time delay may be less detrimental than a decrease, unlike normal conventions [31].

For time delay mismatch, there is no correlation between the original magnitudes of time delay with the magnitude of the resulting overall IAE, unlike gain. However, the magnitudes of overall IAE correspond to the original magnitudes of gain, signifying that the higher the gain, the larger the effect of time delay mismatch on the plant performance. Gain magnitude is found to be the major factor contributing to the increase IAE during time delay mismatch.

### **Plant controllability**

Unlike for gain and time constant, the local minimum for all time delay results are at 0%. From control theory, the plant should be easier to control with lower time delays, but the local minimum does not reflect that here, signifying that the model residuals have a far greater effect on the plant performance for time delay mismatch.

### **Plant step response analysis**

The step responses show that the oscillation of the plant output increases as time delay mismatch increases. Both negative and positive mismatch produces an oscillatory and vigorous response.

It can be observed from figure 20, there are 2 local peaks at about +35% mismatch and -35% mismatch. This shows that a certain amount of time delay mismatch there effects would resonate cause high IAE due to vigorous oscillations. The result from Ali et al. also point towards the presence of several stable and unstable regions within a time delay plane [32]. An example of the response can be seen in figure 21, which shows the output for -35% Delay22 mismatch. These oscillations are more vigorous than in the output for -40% Delay22 mismatch, as shown in figure 22. This vigorous oscillatory behavior is the reason the IAE graphs of time delay mismatch are not smooth.

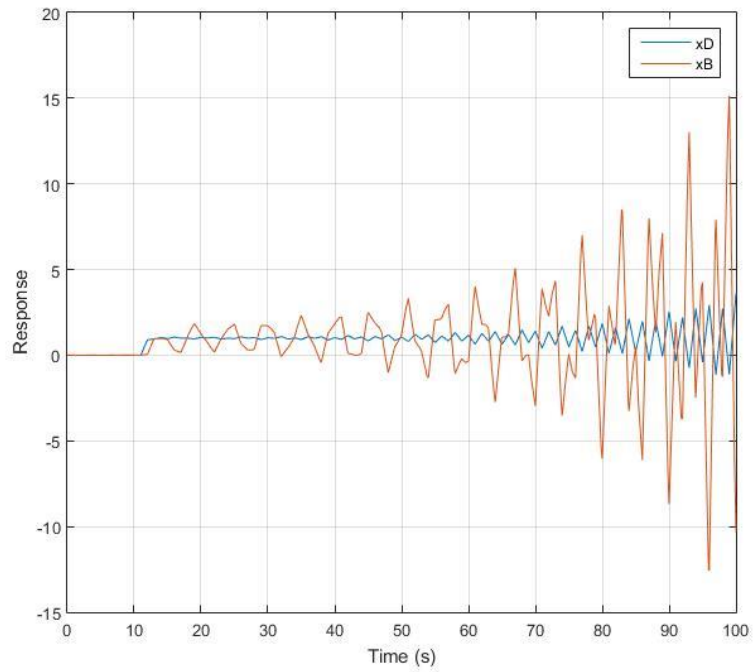


Figure 21: Output response for -35% Delay22 mismatch

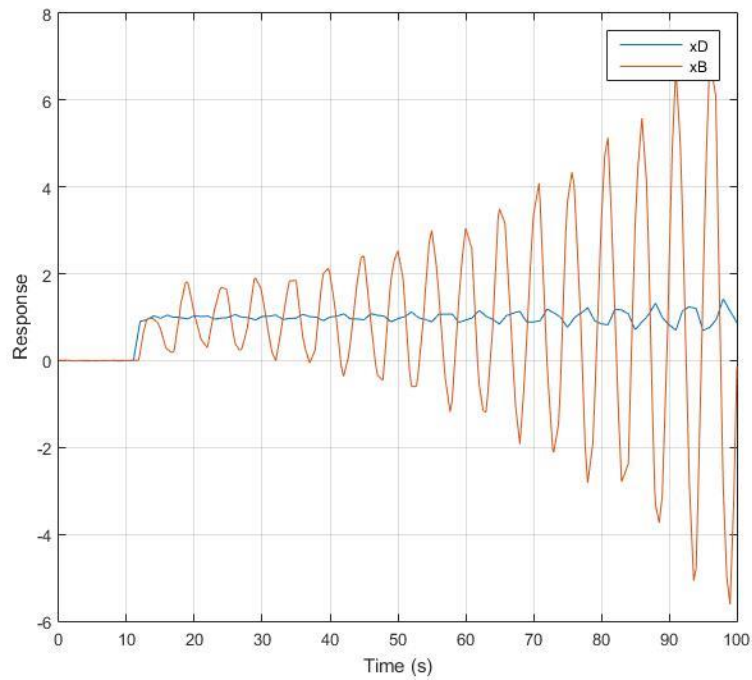


Figure 22: Output response for -40% Delay22 mismatch

#### 4.1.4 bSingle parameter mismatch threshold

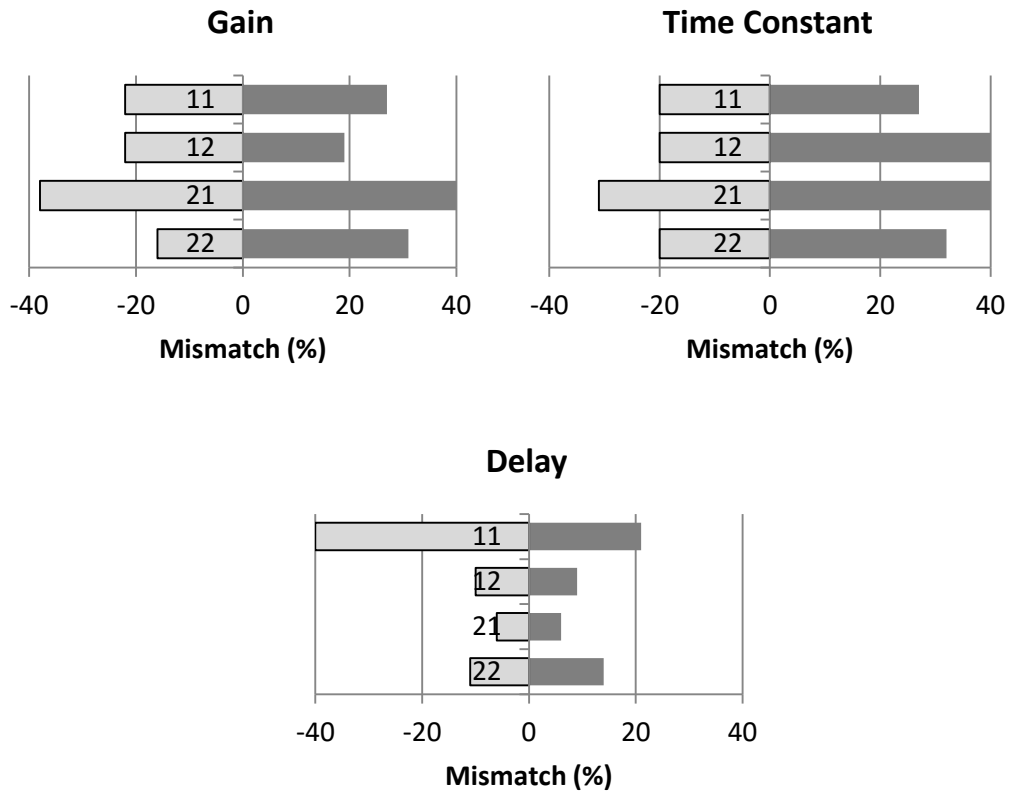


Figure 23: Mismatch thresholds

#### Single gain mismatch

It is noted that  $x_B$  generally has a higher IAE when compared to  $x_D$  in all trials. From figure 11, it can be seen that the IAE for  $x_B$ , though unchanging is still almost always higher than the IAE for  $x_D$ . This observation makes using a fixed IAE, ITAE or ISE threshold to determine the threshold of mismatch unreliable. Therefore, a percentage increase in output error should be employed as a significance threshold, taking into account the nature of the responses.

Observing the shape of the graphs, it is determined that the IAE is most suited for determining the mismatch threshold as it shows a clear trend between error and mismatch. Instability of permanent error issues can be detected when the error increases exponentially with mismatch.

The mismatch threshold can thus be set by identifying the corresponding mismatch when the IAE increases by a certain percentage. This is because the IAE directly corresponds to deviations of the output from the set point. In this situation, the percentage is set to 40%. This percentage is more than sufficient to exclude mismatches that cause permanent offset or instability for gain, time constant and time delay. During significant permanent offset, the IAE increases by at least 96% (calculated from the data at -25% Gain22 mismatch). Based on the above criteria, the mismatch threshold can be inferred from the error graphs.

Table 7: Gain mismatch threshold

Gain	+ Threshold (%)	- Threshold (%)
11	27	22
12	19	22
21	40	38
22	31	16

The threshold values for Gain11, Gain12 and Gain22 conforms to the trend of condition numbers, where the threshold is larger in the direction of decreasing condition numbers. Gain21 is an exception, probably due to having only a small change in condition number across the mismatch scale. However, this discrepancy proves that although the condition number gives a good indication on the direction in which the threshold would lean, it is not the only factor affecting the plant performance.

### Single time constant mismatch

Similar to gain, the mismatch threshold will be determined by limiting the increase in IAE to 40%. Since all responses of time delay mismatch are stable and return to the set point within the simulation duration, instability issues are not of concern.

Table 8: Time constant mismatch threshold

Time constant	+ Threshold (%)	- Threshold (%)
11	27	20
12	40	20
21	40	31
22	32	20

It can be seen from the threshold values that the positive threshold is always larger than the negative threshold; this is due to higher IAE when the response oscillates during negative percentage time constant mismatch.

These threshold span are also quite similar to gain threshold, thus it can be inferred that mismatches in gain and time constant have similar degrees of impact on the plant performance.

### Single time delay mismatch

The time delay mismatch threshold will be determined by limiting the increase in IAE to 40%. This criterion will avoid all unstable oscillatory responses as those would result in at least a 300% increase in IAE.

Table 9: Time delay mismatch threshold

Time delay	+ Threshold (%)	- Threshold (%)
11	21	40
12	9	10
21	6	6
22	14	11

Comparing the threshold values with those of gain and time constant, it can be seen that the threshold are much tighter. This indicates that time delay has a much greater effect on plant performance and thus can only tolerate small mismatches.

## 4.2 Double Parameter Mismatch

Double parameter mismatch refers to having two transfer function components, either gain, time constant or time delay mismatched at the same time. This section puts emphasis on their interactions and consequent effect on IAE as well as how those interactions affect the mismatch thresholds that are determined previously. Surface plots are generated where the x and y axis represents mismatch in two transfer function parameters and the z axis represents the IAE.

### Common trends

Two trends are universal throughout the results. The 1<sup>st</sup> deals with the cumulative nature of the mismatch. This causes the surface plots to be bowl shaped, where high IAE is found at the vertices and edges and the lowest IAE is found near the center. Usually, there would be a direction where the IAE is magnified and this forms a local peak. This peak varies for each trial and always occurs at one of the vertices, where the mismatch is the highest. An example can be seen in figure 24. However, there are instances during high time delays mismatch that yields local peaks not at the vertex of the surface plots, caused by resonance of the. This irregularity however, it not present within the threshold limits determined in section 4.1.4.

The second inclination is similar to the trend found in the single mismatch section, where mismatch of a transfer function that affects one output has insignificant effect on the other output. This type of response can be seen in figure 25. It is observed that  $x_D$  is significantly affected by Gain11 only, as seen by the shape that is raised at the extremes of Gain11 mismatch. The same trend is seen for  $x_B$  with Gain21. Interaction effects are only significant in the direction of increasing condition number that is -40% Gain11 and +40% Gain21, where the IAE is magnified.

In the following parts of this section, the interactions discussed would always involve parameters of transfer function that affect the same output. The ones which affect different outputs have the same trends and thus been generalized above.

### 4.2.1 Double gain mismatch

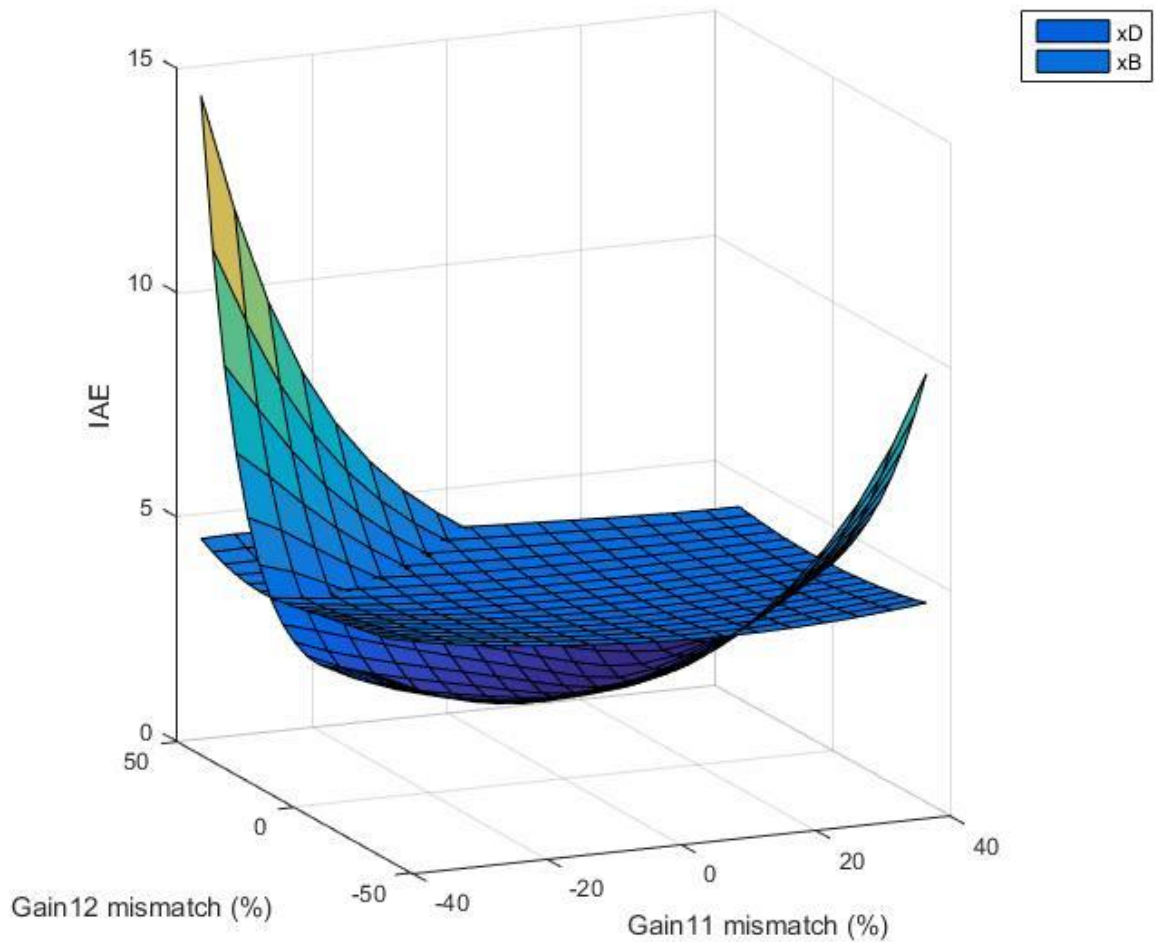


Figure 24: Gain11 and Gain12 mismatch IAE

For double gain mismatch, the interactions are only significant when the gains contribute to a single output, such as in figure 25, where Gain11 and Gain21 are varied.

For  $x_D$  the IAE is the highest for -40% Gain11 mismatch and +40% Gain12 mismatch, this point corresponds to the trend of condition numbers. Decreasing Gain11 and increasing Gain12 makes the plant more difficult to control. Thus, it is established that the mismatch effects are magnified in the direction of increasing condition numbers for the respective gains.

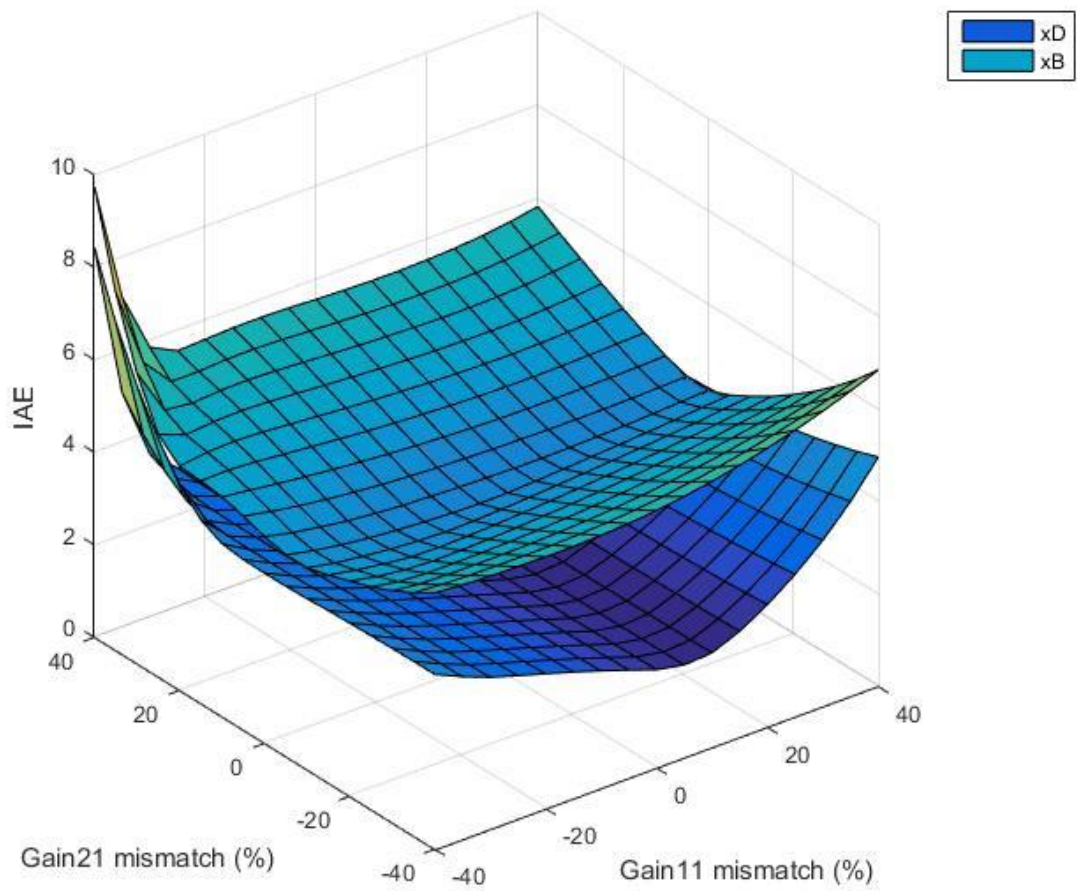


Figure 25: Gain11 and Gain21 mismatch IAE

It is interesting to note that at the opposite vertex of the surface, where the plant is supposedly easy to control, there is also a peak in IAE. This peak however, is not as high as the peak where the plant becomes the hardest to control. This trend is also observed for the combination of Gain21 and Gain22. Thus, it can be inferred that when the magnitude gains are increased or decreased in tandem, the IAE is small. The reason for magnification and nullification is further explained in section 4.2.3.

#### 4.2.2 Double time constant mismatch

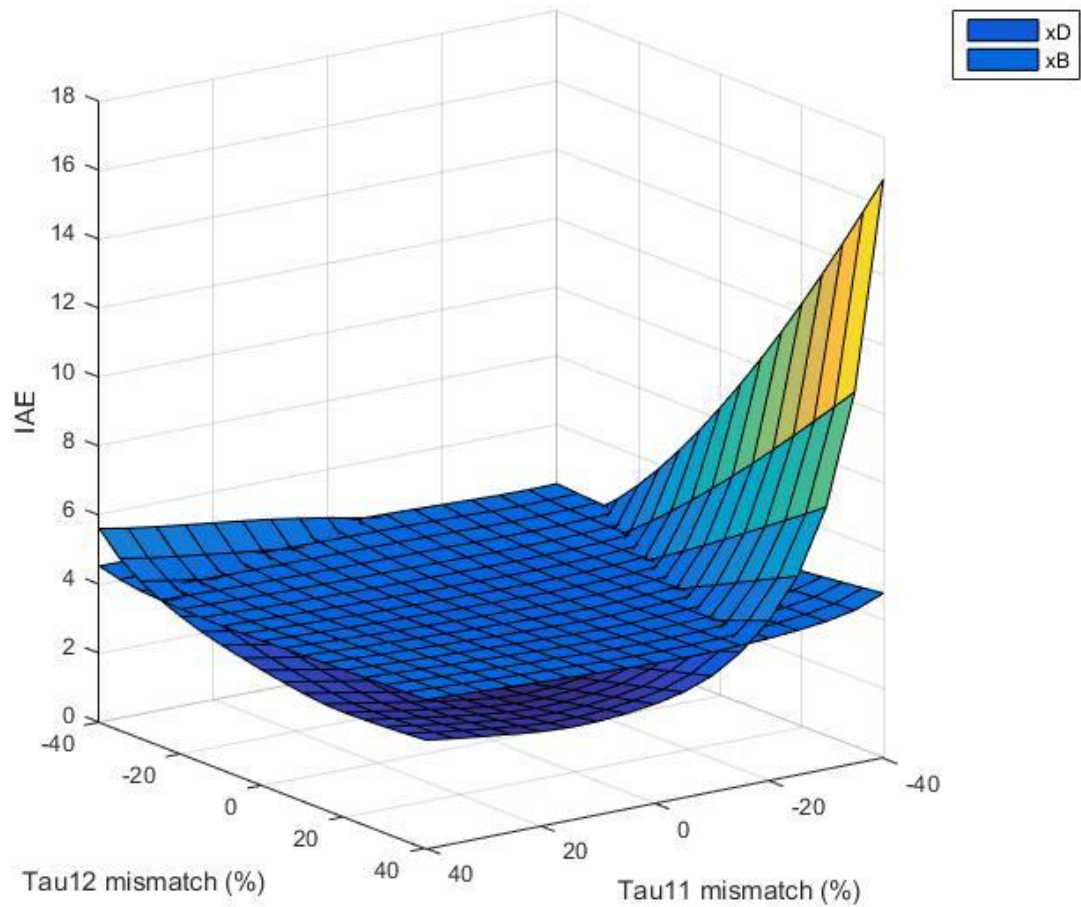


Figure 26: Tau11 and Tau12 mismatch IAE

Similar to double gain mismatch, the interaction effect is only significant when the time constants varied contribute to the same output, as in figure 26 (Tau11 and Tau12). For  $x_D$  the IAE is the highest for -40% Tau11 mismatch and +40% Tau12 mismatch, this does not match the criteria set in the previous part where negative time constant mismatch yield higher IAE. It is interesting to note that the IAE is comparatively low at -40% Tau11 and -40% Tau12 mismatch, suggesting some nullification of effects. Since the results for the combination of Tau12 and Tau22 exhibits the same trend, it can be inferred that the increase or decrease of the time constants in tandem will yield less IAE than if they are displaced in the

opposite direction. The highest peak however, always happens at -40% of the time constant with the larger impact, as determined in section 4.1.4.

### 4.2.3 Double time delay mismatch

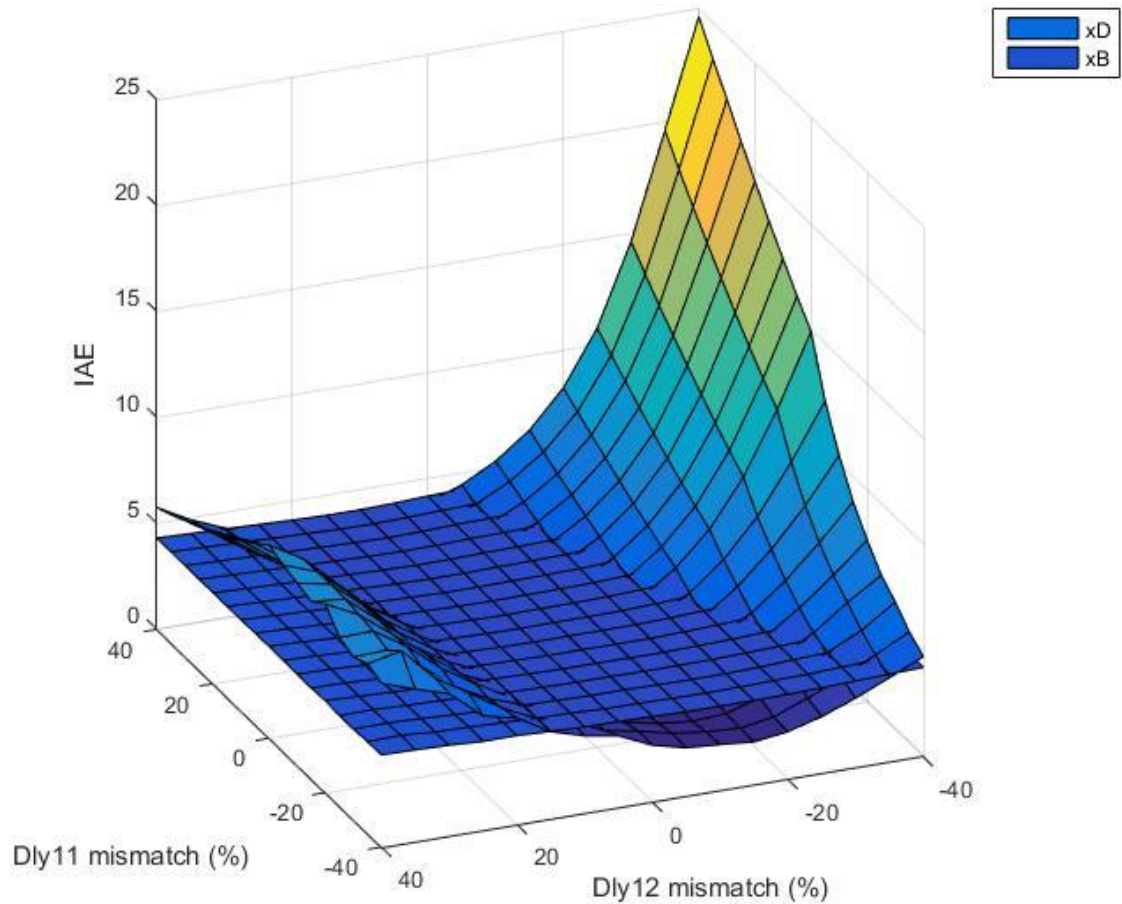


Figure 27: Delay11 and Delay12 mismatch IAE

Significant interaction can also only be observed for time delay mismatches that contribute to the same output, as shown in figure 27 (Delay11 and Delay12). At high mismatch values, there are some resonant spots with higher IAE than at the edges, where the IAE shoots up drastically. For  $x_D$  the IAE is the highest for +40% Delay11 mismatch and -40% Delay12 mismatch, this does not correspond to the determined degree of impact for the time constants as can be seen in section 4.1.4.

Similar to gain and time constant, it is found that the increase or decrease of the time delays in tandem will yield less IAE than if they are displaced in the opposite direction.

The phenomena where nullification effects are present when either double gain, double time constant and double time delay is increased or decreased in tandem can be explained if we study the effect the mismatch has on the transfer functions involved. An increase in gain, decrease in time constant or decrease in time delay increases the effect of a transfer function and vice versa. Thus, increasing both gains of the two transfer functions will increase the effect of both transfer functions together. Their relative difference would be small and thus the IAE is small. On the other hand, increasing one gain and decreasing the other will increase their relative difference and cause high IAE. The same holds true for time constant and time delays. This effect will be referred to as the imbalance between two transfer functions.

This inference is further strengthened when the direction that will supposedly give high IAE based on the directions of severe effect as determined in the single parameter section, gives low IAE instead. One good example is -40% Tau11 and -40% Tau12 as seen in figure 26, which gives low IAE despite both being the direction with the lower threshold.

#### 4.2.4 Gain and time constant mismatch interaction

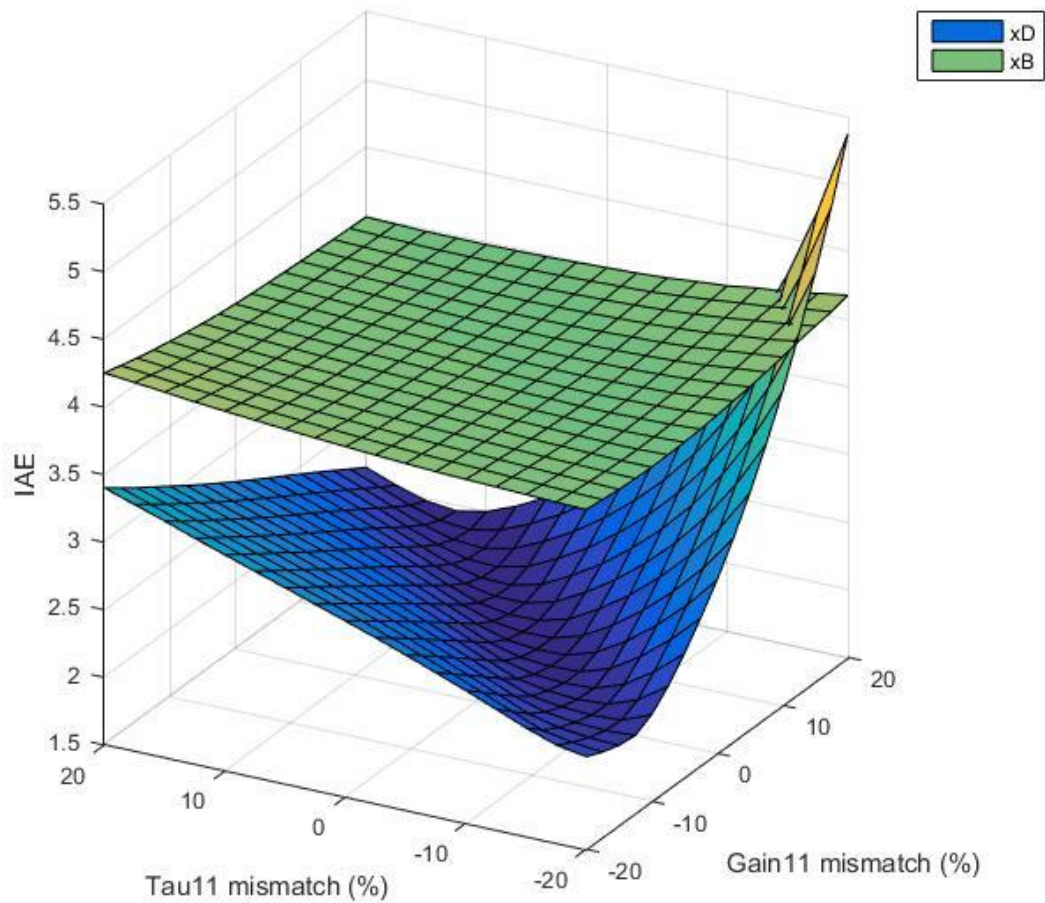


Figure 28: Gain11 and Tau11 mismatch IAE

From this section onwards, the mismatch matrix is defined from only -20% to +20% because high interactions prevent the trend to be clearly seen with a larger matrix.

For gain and time constant, there are generally two types of combinations. For the first type, the gain and time constant from the same transfer function are varied (Gain11 and Tau11). The results can be seen in figure 28, where the highest peak occur at +20% Gain11, -20% Tau11. For the second type, the gain and time constant from different transfer functions but affecting the same output are varied

(Gain11 and Tau12). The result is shown in figure 29. The highest peak is found in -20% Gain11 and -20% Tau12.

The trends can be explained using the balance between transfer functions. For the first combination, increasing the gain and decreasing the time constant for transfer function 11 will increase its relative difference with transfer function 12, which will then cause high IAE. For the second combination, increasing or decreasing the parameters in tandem will increase the relative difference.

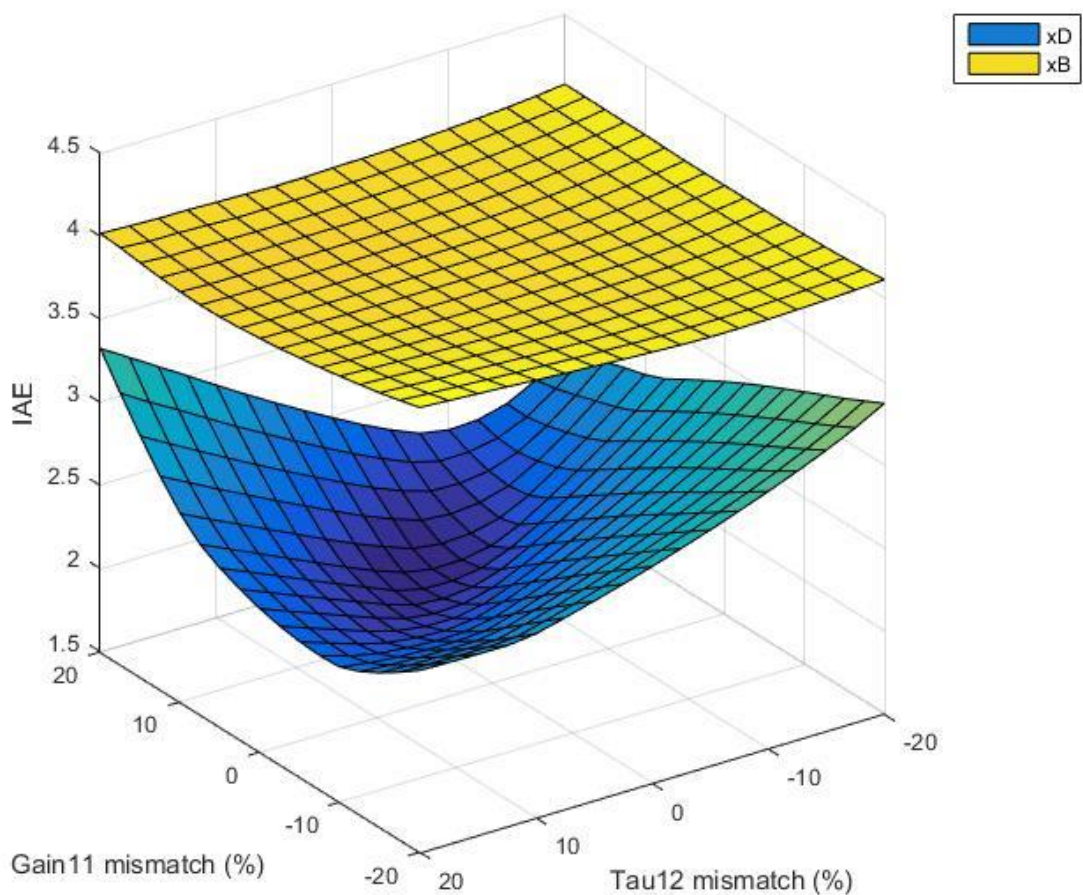


Figure 29: Gain11 and Tau12 mismatch IAE

#### 4.2.5 Gain and time delay mismatch interaction

For the interaction between gain and delay that affect the same output, the trend is the same regardless if it is from the same transfer function (Gain11 and

Delay11) or different (Gain11 and Delay12). From figure 30, it can be observed that the IAE depends more on time delay mismatch, which is more dominant in this system. The surface curves more along the time delay axis. In the direction of adverse time delay mismatch, the highest peak is always towards positive gain mismatch. This may be because an increase in gain mismatch makes the response more oscillatory, which magnifies the effect of time delay mismatch.

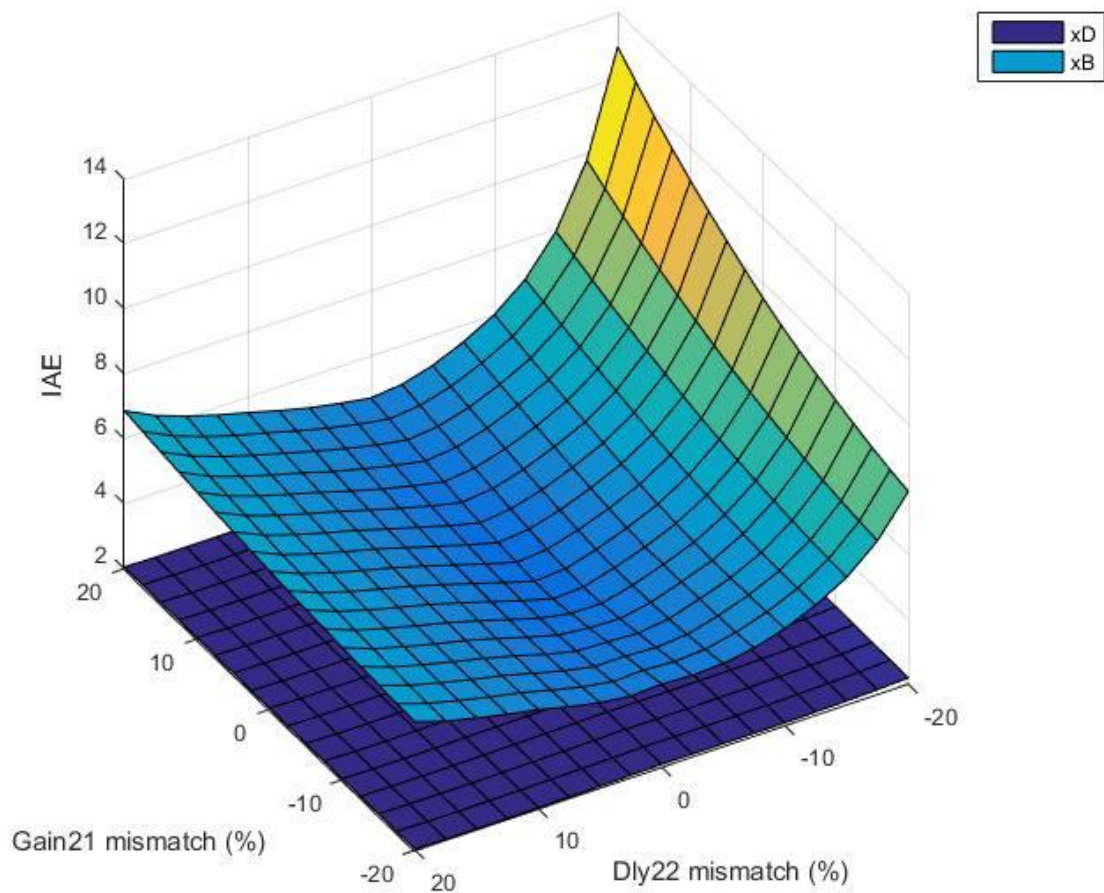


Figure 30: Gain21 and Delay22 mismatch IAE

#### 4.2.6 Time constant and time delay mismatch interaction

For the interaction between time constant and delay that affect the same output, the trend is the same regardless if it is from the same transfer function (Tau11 and Delay11) or different (Tau11 and Delay12).. From figure 31, it can be

observed that the IAE depends more on time delay mismatch, which is more dominant in this system. In the direction of adverse time delay mismatch, the highest peak is always towards negative time constant mismatch. This is because negative time constant mismatch yields higher IAE due to the more oscillatory response, as seen in the results in single time constant mismatch.

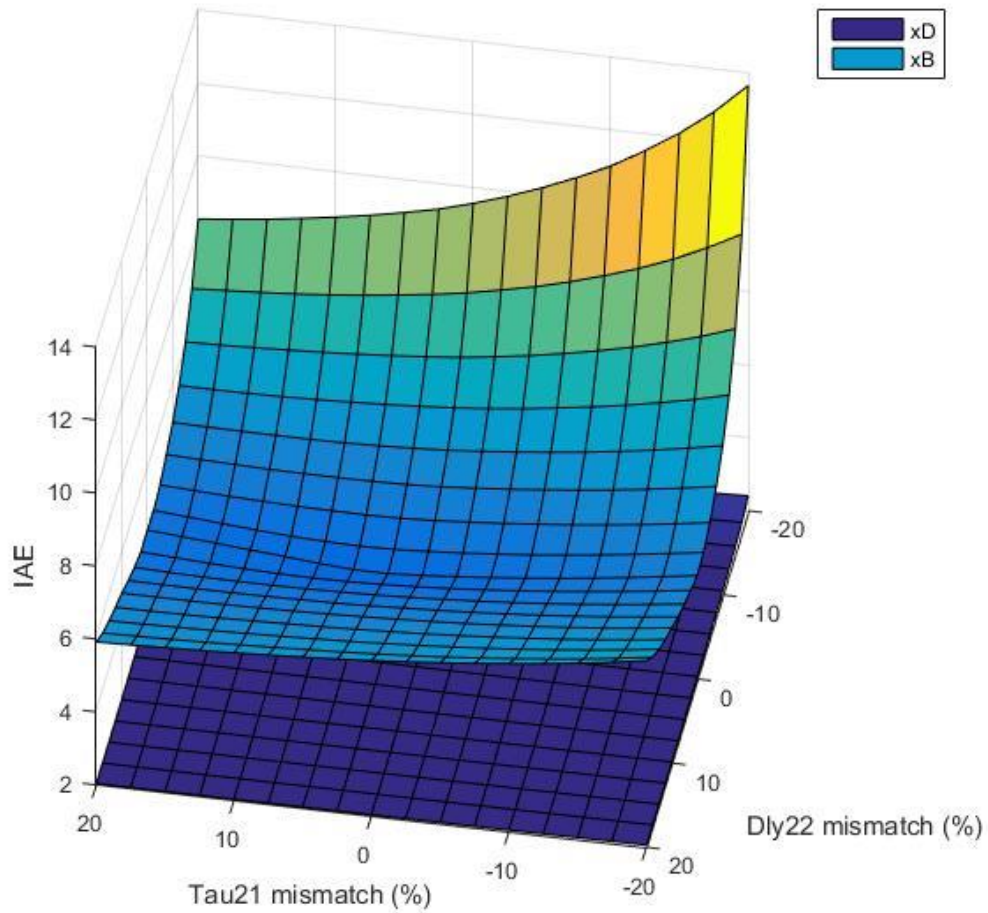


Figure 31: Tau21 and Delay22 mismatch IAE

#### 4.2.7 Double parameter mismatch threshold considerations

When there are two mismatched gains, time constant or time delay the threshold as determined in the single variable part are not be applicable because of the interaction effects. Here, the threshold is tested in the direction of the highest IAE peak where the directions cause an imbalance between the transfer functions involved, as defined in section 4.2.3. For double gain, this occurs where the condition numbers increases for both gains since the other directions will yield lower IAE. For double time constant and double time delay, this occurs when the time constants or time delays are displaced in the opposite directions.

For one gain and one time constant mismatch, the peak also occurs when the direction causes an imbalance. For interactions involving time delay and the other parameter being gain or time constant, the IAE is generally higher in the direction of adverse time constant mismatch, accompanied by positive gain or negative time delay mismatch.

For mismatched parameters that contribute to the same output, the interactions are cumulative and large, thus, maintaining the threshold will not guarantee the IAE increase of less than +40% as needed. From the results, it is found that the positive threshold for Gain12 and negative threshold for Gain11 must be halved in order ensure that the IAE is within limits for a combination of Gain11 and Gain12 mismatch. This technique of halving thresholds is found to be sufficient to ensure the IAE is within limits for all other dual parameter mismatches of the same nature.

For mismatched parameters that contribute to different outputs, the interactions are not large. Maintaining the thresholds is sufficient to prevent IAE from exceeding the limit. Thus, for the second type, the thresholds can be maintained, assuming slight over limits of IAE increase can be tolerated.

## **4.3 Results Summary**

### **4.3.1 Single parameter mismatch**

As a summary, gain and time constant have comparable effects on the IAE of this system while time delay has a much more severe impact. The direction of mismatch that yields higher IAE depends on plant condition number for gain but is constantly negative for time constant. This trend can be clear seen from the mismatch thresholds found. For time delay, the pattern is not apparent and the threshold is much smaller.

Observing the magnitude of the original gains will show which mismatch in gain or time delay will generally yield higher IAE. For time constant, there is no trend. The shape of the graph for gain and time constant will also provide information on the plant response. An sharp increase usually points towards instability or high IAE, while a smaller slope points towards lower IAE levels. For time delay, since the effect is so severe, the shape is irregular due to high oscillations.

### **4.3.2 Double parameter mismatch**

Interactions between the mismatches are high when the parameters mismatch coincides with the transfer functions that contribute to the same output. For example, mismatch in transfer function 11 and 12 or transfer function 21 and 22. Interactions are low when the mismatch coincides with transfer functions that affect different outputs. For example, transfer function 11 and 21 or 11 and 22. High interactions mandates the threshold determined in section 4.1.4 to be half while low interactions permits the threshold to remain.

If the relative difference between the transfer functions increases due to a combination of mismatch direction, the IAE will magnify. On the other hand, there will be nullification effects when the combination retains their relative difference. This trend is true for double gain, double time constant, double time delay and gain with time delay.

For combinations of time delay with gain or time delay with time constant, there are no nullification effects. The shape curves with time delay mismatch, with the highest peak occurring at negative time constant and positive gain respectively.

## **CHAPTER 5**

### **CONCLUSION AND RECOMMENDATIONS**

#### **5.1 Conclusion**

The relationship between model-plant mismatch and plant performance is quantified from -40% to +40% of parametric mismatch. All gain mismatch directions have IAE that increases steadily with mismatch for the distillation model studied except for negative Gain22 mismatch, which shows a sharp increase. For time constant mismatch, the IAE slope is steeper for negative mismatch. The trend for time delay is irregular but maintains generally an increase, increase relationship.

The threshold of mismatch is determined by limiting the IAE increase by 40% of the base IAE at 0% mismatch. The thresholds for gain are larger in the direction of decreasing plant condition number. For time constant, positive mismatch has higher thresholds. The thresholds for time delay are generally much smaller than time constant and gain but do not show preferences for either direction.

Mismatch parameters interact when they are present in transfer functions directly contributing to one output. For double gain, double time constant, double time delay and gain with time constant, the performance drop is magnified when the combination of mismatch increase the relative difference between the transfer functions involved. Time delay dominates the interaction when present with either time constant or gain.

In the presence of dual mismatch, the threshold determined from single parameter mismatch should be halved. This will ensure the IAE does not increase beyond 40% in the direction of highest magnification due to interactions.

## 5.2 Recommendations

Further expansion of the research should include a study of other multiple input multiple output systems to ensure validity of the trends in other models. The threshold determined should also be tested with a case study of a model utilizing available mismatch estimation techniques to determine the effectiveness of the value.

To further understand interactions with more than two mismatches, simulation studies can be done. Critical mismatch directions as determined in section 4.2 of this report can be tested. The effect of those interactions on the threshold should also be studied. The parameters used in the study is fixed, therefore the effect of those parameters on the final graphs and threshold values are unclear.

## REFERENCES

- [1] D. E. Seborg, T. F. Edgar, and D. A. Mellichamp, *Process Dynamics and Control*, 2nd ed. MA, US: John Wiley & Sons, 2004.
- [2] J. S. Conner and D. E. Seborg, "Assessing the Need for Process Re-identification," *Industrial & Engineering Chemistry Research*, vol. 44, pp. 2767-2775, 2005/04/01 2005.
- [3] M. Morari and J. H. Lee, "Model predictive control: past, present and future," *Computers & Chemical Engineering*, vol. 23, pp. 667-682, 5/1/ 1999.
- [4] J. Schäfer and A. Cinar, "Multivariable MPC system performance assessment, monitoring, and diagnosis," *Journal of Process Control*, vol. 14, pp. 113-129, 3// 2004.
- [5] H. Wang, L. Xie, and Z. Song, "A Review for Model Plant Mismatch Measures in Process Monitoring," *Chinese Journal of Chemical Engineering*, vol. 20, pp. 1039-1046, 12// 2012.
- [6] G. McMillan and S. Weiner. (2013, 14th June, 2015). Model Predictive Control - Past, Present and Future.
- [7] S. Selvanathan and A. K. Tangirala, "Diagnosis of Poor Control Loop Performance Due to Model-Plant Mismatch," *Industrial & Engineering Chemistry Research*, vol. 49, pp. 4210-4229, 2010/05/05 2010.
- [8] M. Jelali, "An overview of control performance assessment technology and industrial applications," *Control Engineering Practice*, vol. 14, pp. 441-466, 5// 2006.
- [9] S. L. Jämsä-Jounela, R. Poikonen, N. Vatanski, and A. Rantala, "Evaluation of control performance: methods, monitoring tool and applications in a flotation plant," *Minerals Engineering*, vol. 16, pp. 1069-1074, 11// 2003.
- [10] T. J. Harris, "Assessment of control loop performance," *The Canadian Journal of Chemical Engineering*, vol. 67, pp. 856-861, 1989.
- [11] B. Huang, S. L. Shah, and K. Y. Kwok, "Good, bad or optimal? Performance assessment of MIMO processes," *Automatica*, vol. 33 (6), pp. 1175-1183, 1997.
- [12] H. Wang, Z. Song, and L. Xie, "Parametric Mismatch Detection and Isolation in Model Predictive Control System," *Preprints of the 8th IFAC Symposium on Advanced Control of Chemical Processes, The International Federation of Automatic Control*, 2012.
- [13] F. Yin, H. Wang, L. Xie, P. Wu, and Z. Song, "Data driven model mismatch detection based on statistical band of Markov parameters," *Computers & Electrical Engineering*, vol. 40, pp. 2178-2192, 10// 2014.
- [14] S. Kaw, A. K. Tangirala, and A. Karimi, "Improved methodology and set-point design for diagnosis of model-plant mismatch in control loops using plant-model ratio," *Journal of Process Control*, vol. 24, pp. 1720-1732, 11// 2014.
- [15] A. S. Badwe, R. S. Patwardhan, S. L. Shah, S. C. Patwardhan, and R. D. Gudi, "Quantifying the impact of model-plant mismatch on controller performance," *Journal of Process Control*, vol. 20, pp. 408-425, 4// 2010.
- [16] G. Vinnicombe, "The v-gap metric," in *Uncertainty and Feedback*, ed, 2000, pp. 104-166.
- [17] S. Wan and B. Huang, "Robust performance assessment of feedback control systems," *Automatica*, vol. 38, pp. 33-46, 1// 2002.

- [18] H. Jiang, W. Li, and S. L. Shah, "Detection and Isolation of Model-Plant Mismatch for Multivariate Dynamic Systems," in *Fault Detection, Supervision and Safety of Technical Processes 2006*, H.-Y. Zhang, Ed., ed Oxford: Elsevier Science Ltd, 2007, pp. 1396-1401.
- [19] A. S. Badwe, R. D. Gudi, R. S. Patwardhan, S. L. Shah, and S. C. Patwardhan, "Detection of model-plant mismatch in MPC applications," *Journal of Process Control*, vol. 19, pp. 1305-1313, 9// 2009.
- [20] M. Kano, Y. Shigi, S. Hasebe, and S. Ooyama, "Detection of Significant Model-Plant Mismatch from Routine Operation Data of Model Predictive Control System," *Proceedings of the 9th International Symposium on Dynamics and Control of Process Systems*, 2010.
- [21] J. R. Webber and Y. P. Gupta, "A closed-loop cross-correlation method for detecting model mismatch in MIMO model-based controllers," *ISA Transactions*, vol. 47, pp. 395-400, 10// 2008.
- [22] G. Ji, K. Zhang, and Y. Zhu, "A method of MPC model error detection," *Journal of Process Control*, vol. 22, pp. 635-642, 3// 2012.
- [23] P. Kesavan and J. H. Lee, "Diagnostic Tools for Multivariable Model-Based Control Systems," *Industrial & Engineering Chemistry Research*, vol. 36, pp. 2725-2738, 1997/07/01 1997.
- [24] B. Huang, "On-line closed-loop model validation and detection of abrupt parameter changes," *Journal of Process Control*, vol. 11, pp. 699-715, 12// 2001.
- [25] L. C. Kammer, D. Gorinevsky, and G. A. Dumont, "Semi-intrusive multivariable model invalidation," *Automatica*, vol. 39, pp. 1461-1467, 8// 2003.
- [26] S. J. Kendra and A. Çinar, "Controller performance assessment by frequency domain techniques," *Journal of Process Control*, vol. 7, pp. 181-194, // 1997.
- [27] C. A. Harrison and S. J. Qin, "Discriminating between disturbance and process model mismatch in model predictive control," *Journal of Process Control*, vol. 19, pp. 1610-1616, 12// 2009.
- [28] L. E. Olivier and I. K. Craig, "Development and application of a model-plant mismatch expression for linear time-invariant systems," *Journal of Process Control*, vol. 32, pp. 77-86, 8// 2015.
- [29] R. K. Wood and M. W. Berry, "Terminal composition control of a binary distillation column," *Chemical Engineering Science*, vol. 28, pp. 1707-1717, 9// 1973.
- [30] V. R. Botelho, J. O. Trierweiler, M. Farenzena, and R. Duraiski, "Assessment of Model-Plant Mismatch by the Nominal Sensitivity Function for Unconstrained MPC," *IFAC-PapersOnLine*, vol. 48, pp. 753-758, // 2015.
- [31] H. Granberg, "Control of a Process with Large Time Constants and Significant Time Delay," Masters in Process Control, Department of Signals and Systems, CHALMERS UNIVERSITY OF TECHNOLOGY, Gothenburg, Sweden, 2013.
- [32] M. S. Ali, Z. K. Hou, and M. N. Noori, "Stability and Performance of Feedback Control Systems with Time Delays," *Worcester Polytechnic Institute*.

# **APPENDICES**

## Matlab code: Single parameter mismatch

```

function [ ] = FYPSimulator( ~ )

load_system('FYP12');

gain11dev_p = [-40:5:40];
gain12dev_p = [-40:5:40];
gain21dev_p = [-40:5:40];
gain22dev_p = [-40:5:40];

hws = get_param('FYP12','modelworkspace');
hws.DataSource = 'MAT-File';
hws.FileName = 'params';

IAEoutputset1 = zeros(1,length(gain11dev_p));
ISEoutputset1 = zeros(1,length(gain11dev_p));
ITAEoutputset1 = zeros(1,length(gain11dev_p));
IAEoutputset2 = zeros(1,length(gain11dev_p));
ISEoutputset2 = zeros(1,length(gain11dev_p));
ITAEoutputset2 = zeros(1,length(gain11dev_p));

for i = 1:length(gain11dev_p)
    hws.assignin('Tau22', gain11dev_p(i));
    hws.saveToSource;

    paramNameValStruct.SaveOutput = 'on';
    paramNameValStruct.OutputSaveName = 'youtNew';
    simOut = sim('FYP12',paramNameValStruct);
    simOut
    IAEoutput = simOut.get('IAEoutput');
    ISEoutput = simOut.get('ISEoutput');
    ITAEoutput = simOut.get('ITAEoutput');

    IAEoutputset1(i) = IAEoutput(1);
    ISEoutputset1(i) = ISEoutput(1);
    ITAEoutputset1(i) = ITAEoutput(1);
    IAEoutputset2(i) = IAEoutput(2);
    ISEoutputset2(i) = ISEoutput(2);
    ITAEoutputset2(i) = ITAEoutput(2);
end

hws.assignin('Gain11', 0);
hws.assignin('Gain12', 0);
hws.assignin('Gain21', 0);
hws.assignin('Gain22', 0);
hws.assignin('Tau11', 0);
hws.assignin('Tau12', 0);
hws.assignin('Tau21', 0);
hws.assignin('Tau22', 0);
hws.assignin('Dly11', 0);
hws.assignin('Dly12', 0);
hws.assignin('Dly21', 0);
hws.assignin('Dly22', 0);

hws.saveToSource;

figure

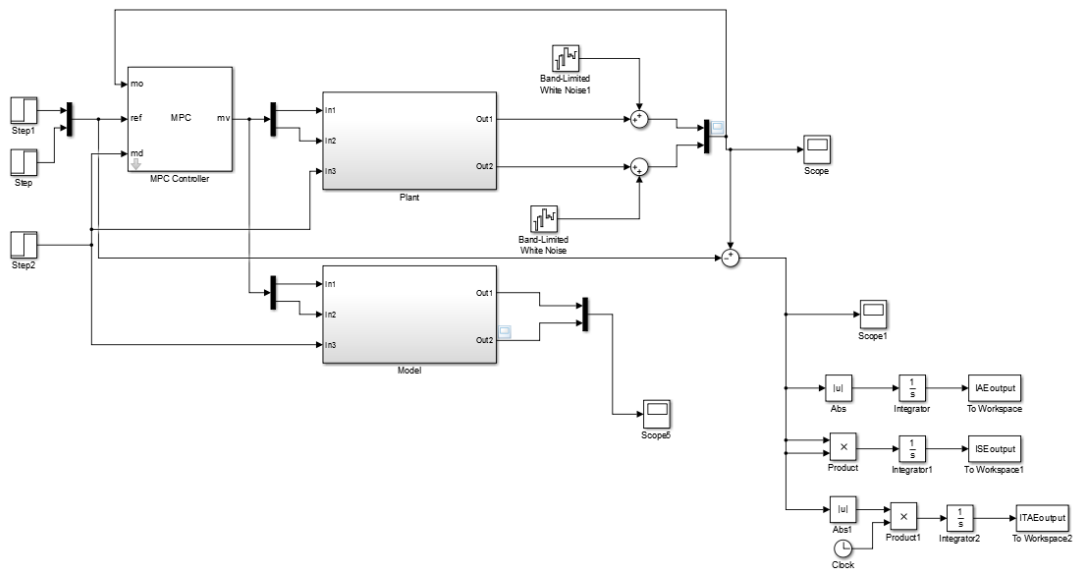
```

```
subplot (2,2,1)
plot(gain11dev_p, IAEoutputset1,gain11dev_p, IAEoutputset2)
xlabel('Deviation(%)')
ylabel('IAE')
legend('xD', 'xB')
hold
subplot (2,2,2)
plot(gain11dev_p, ISEoutputset1,gain11dev_p, ISEoutputset2)
xlabel('Deviation(%)')
ylabel('ISE')
legend('xD', 'xB')

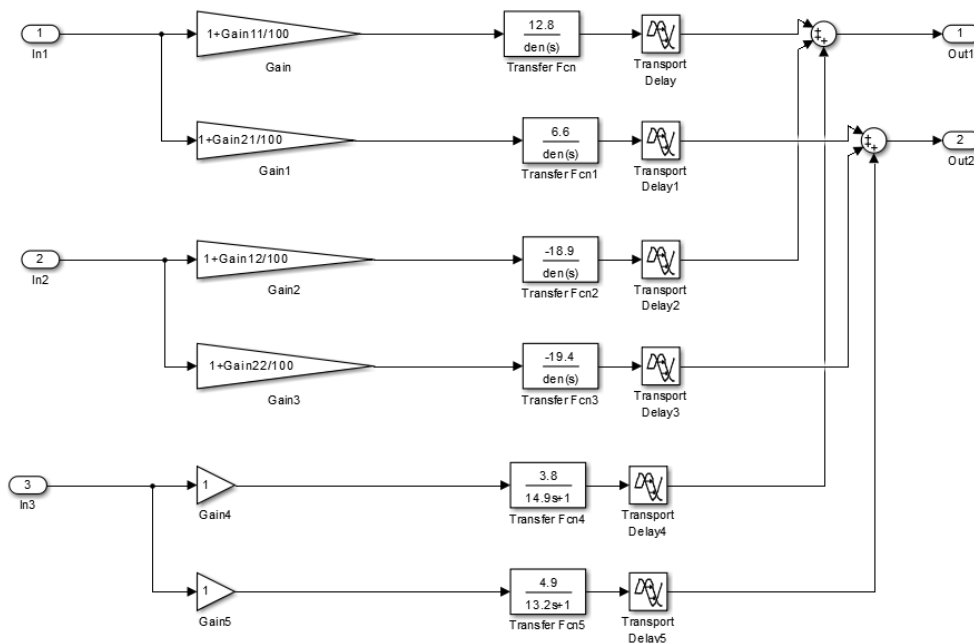
subplot (2,2,3)
plot(gain11dev_p, ITAEoutputset1,gain11dev_p, ITAEoutputset2)
xlabel('Deviation(%)')
ylabel('ITAE')
legend('xD', 'xB')

end
```

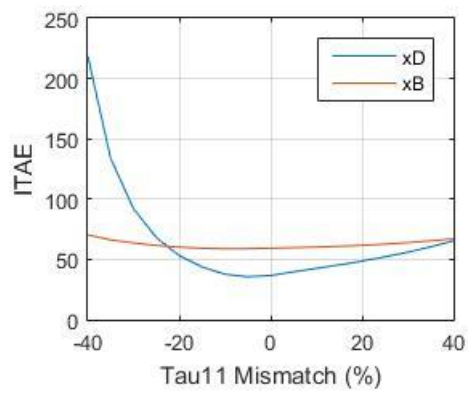
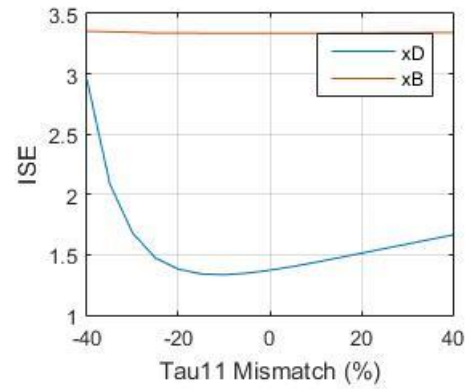
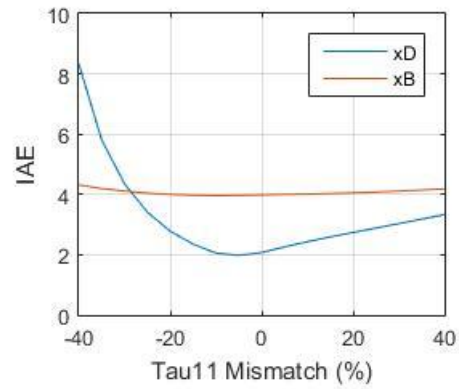
Simulink block diagram



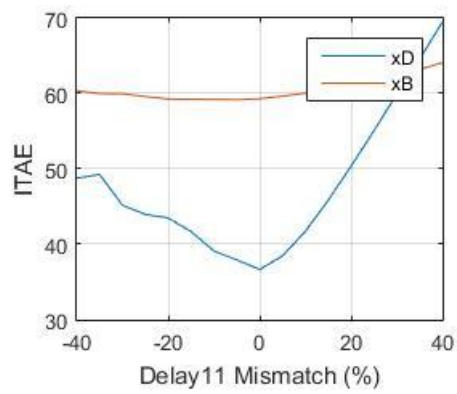
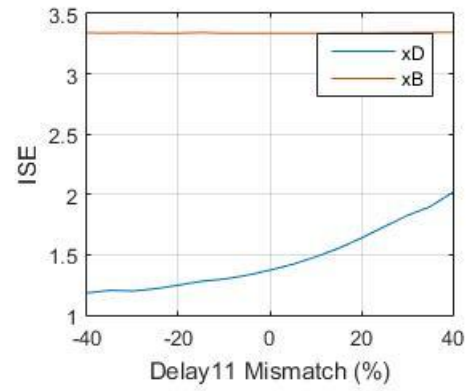
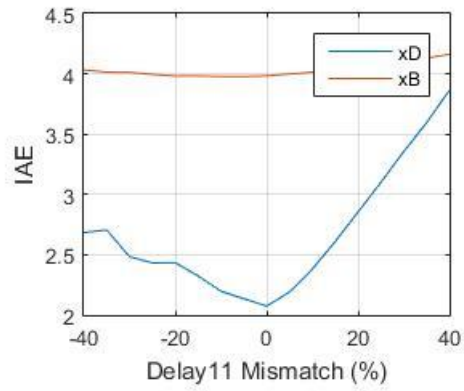
Plant block diagram



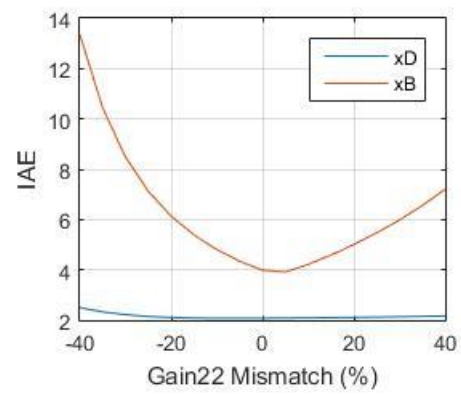
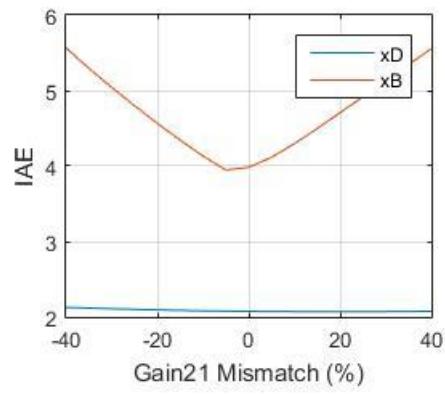
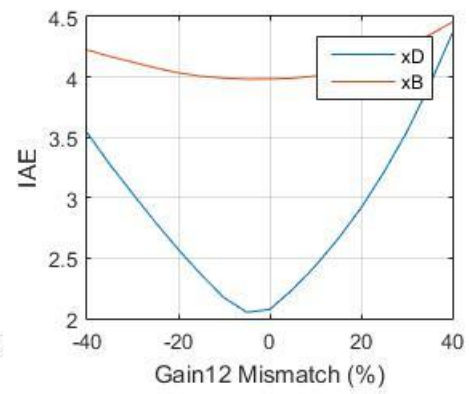
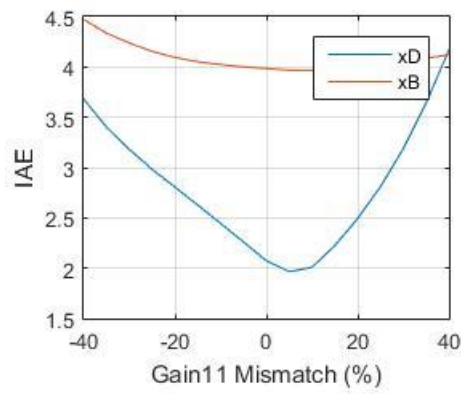
## IAE, ISE and ITAE for Tau11



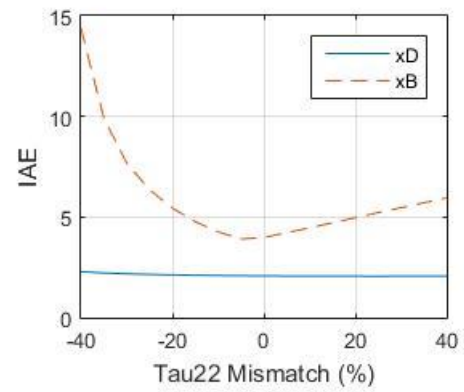
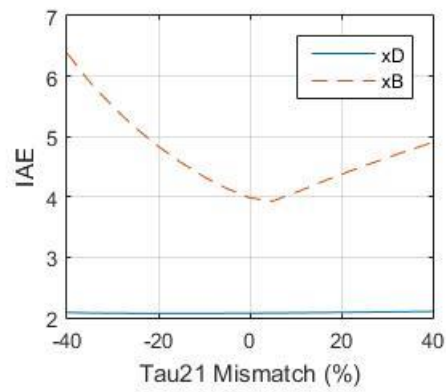
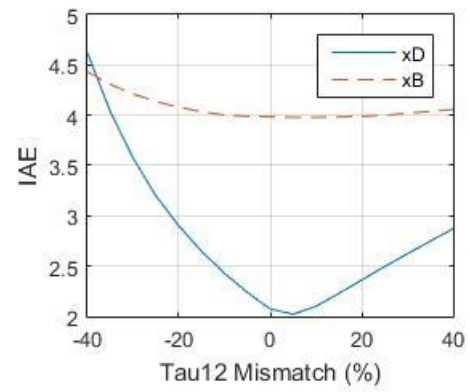
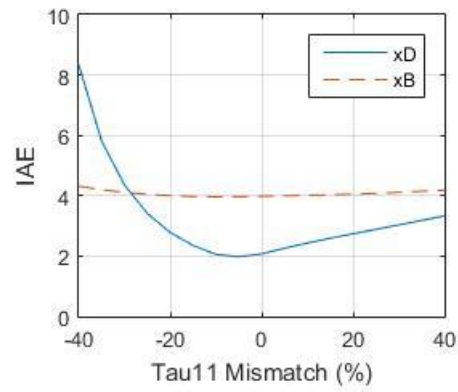
## IAE, ISE and ITAE for Delay11



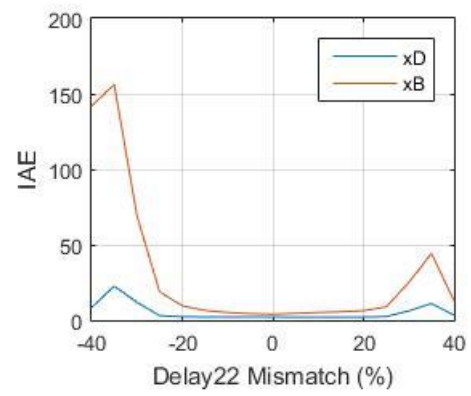
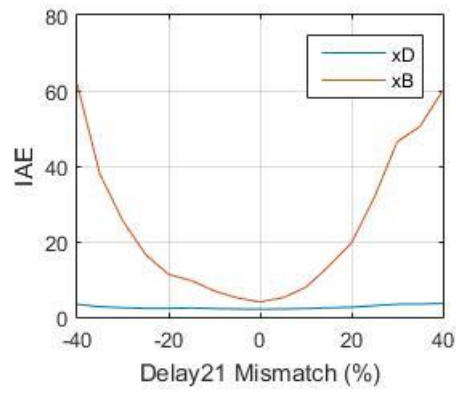
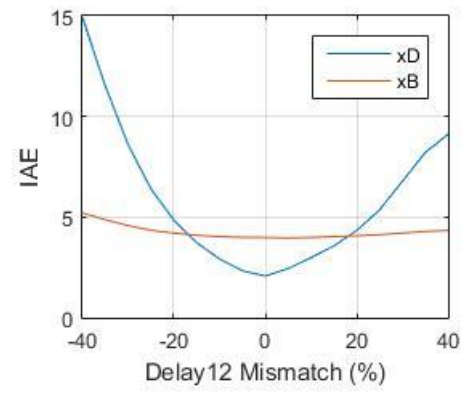
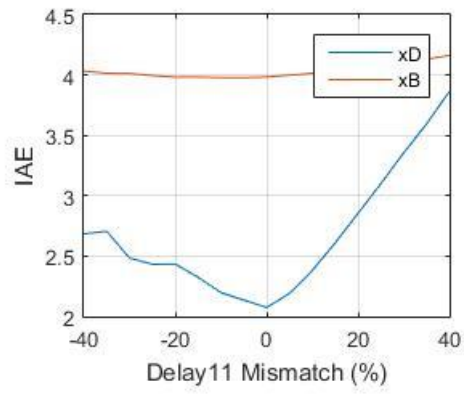
## Results for single gain mismatch



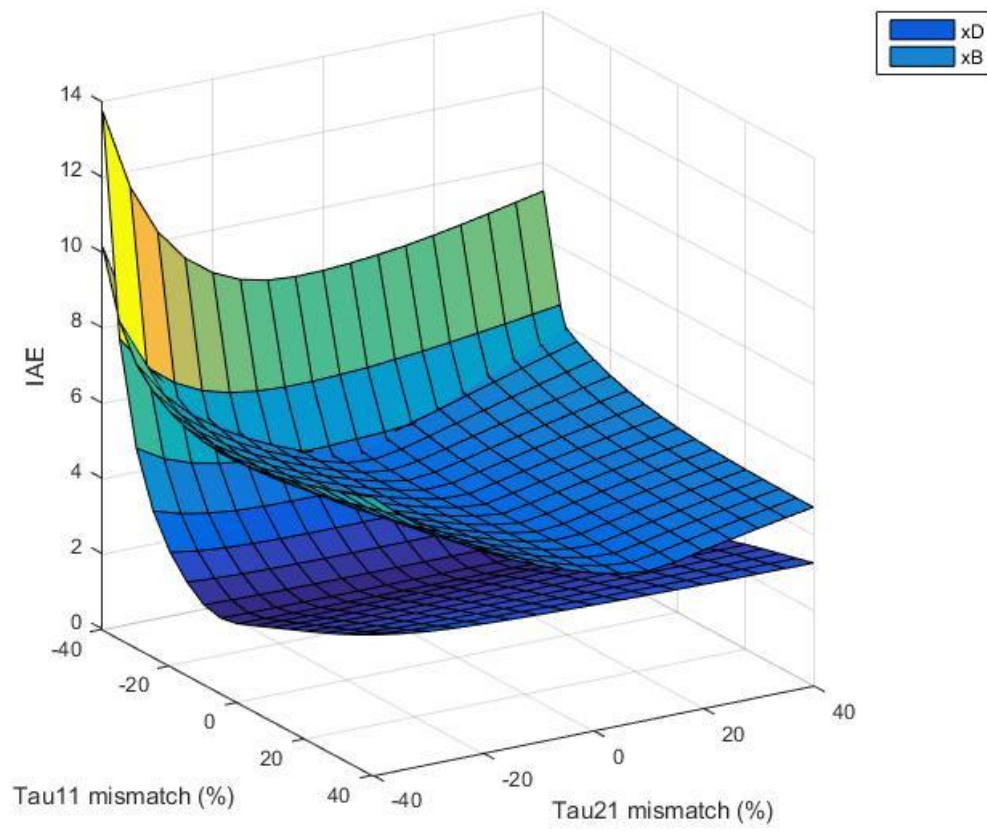
## Results for single time constant mismatch



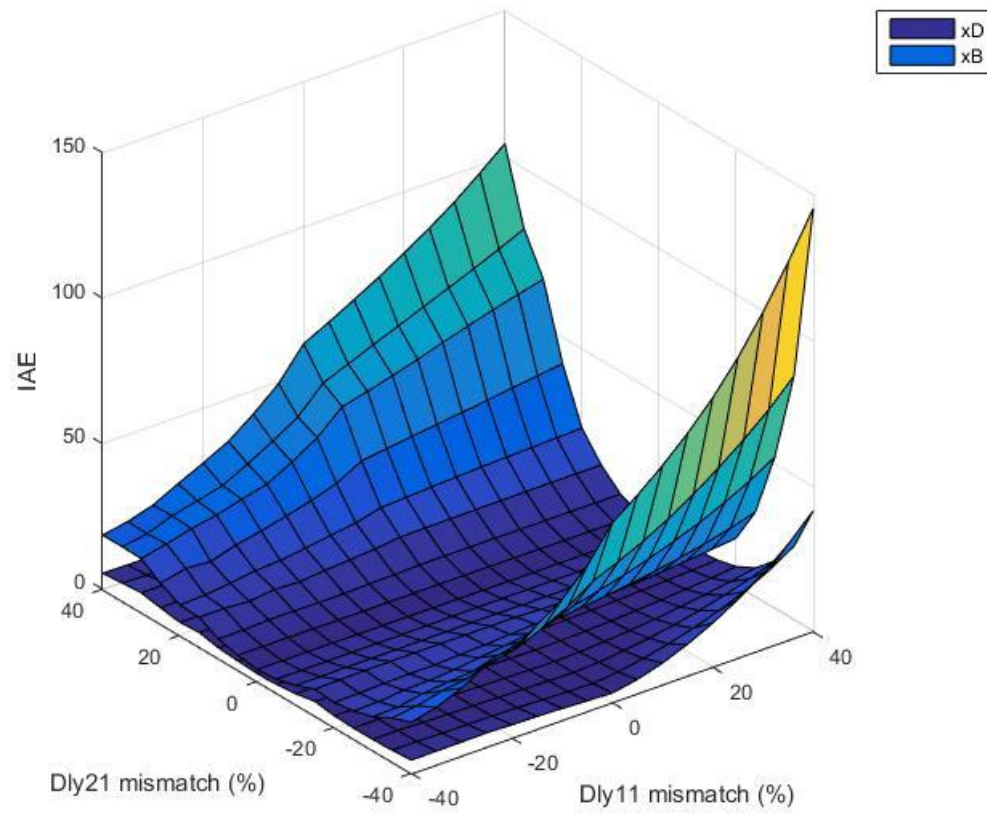
## Results for single time delay mismatch



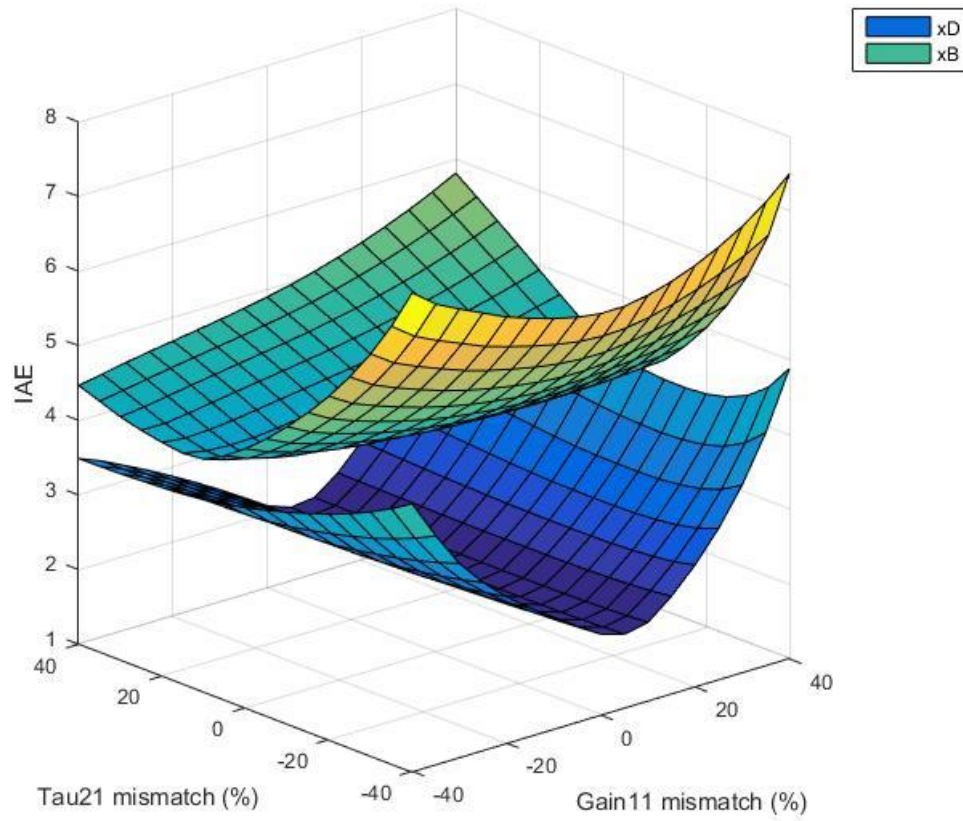
Results for Tau11 and Tau21 interaction (transfer function affecting different outputs)



Results for Delay11 and Delay21 interaction (transfer function affecting different outputs)



Results for Gain11 and Tau21 interaction (transfer function affecting different outputs)



Results for Gain11 and Delay21 interaction (transfer function affecting different outputs)

